

A half-century of rocking isolation

Nicos Makris*

Division of Structures, Department of Civil Engineering, University of Patras, 26500 Patras, Greece

(Received January 23, 2014, Revised May 15, 2014, Accepted May 30, 2014)

Abstract. The uplifting and rocking of slender, free-standing structures when subjected to ground shaking may limit appreciably the seismic moments and shears that develop at their base. This high-performance seismic behavior is inherent in the design of ancient temples with emblematic peristyles that consist of slender, free-standing columns which support freely heavy epistyles together with the even heavier frieze atop. While the ample seismic performance of rocking isolation has been documented with the through-the-centuries survival of several free-standing ancient temples; and careful post-earthquake observations in Japan during the 1940's suggested that the increasing size of slender free-standing tombstones enhances their seismic stability; it was George Housner who 50 years ago elucidated a size-frequency scale effect that explained the "counter intuitive" seismic stability of tall, slender rocking structures. Housner's 1963 seminal paper marks the beginning of a series of systematic studies on the dynamic response and stability of rocking structures which gradually led to the development of rocking isolation—an attractive practical alternative for the seismic protection of tall, slender structures. This paper builds upon selected contributions published during this last half-century in an effort to bring forward the major advances together with the unique advantages of rocking isolation. The paper concludes that the concept of rocking isolation by intentionally designing a hinging mechanism that its seismic resistance originates primarily from the mobilization of the rotational inertia of its members is a unique seismic protection strategy for large, slender structures not just at the limit-state but also at the operational state.

Keywords: seismic protection; rocking frame; recentering; moment of inertia; earthquake engineering

1. Introduction

The design of most structural framing systems is based on three basic concepts which are deeply rooted in modern structural engineering. The first concept is that of creating statically indeterminate (redundant) framing systems. When an "indeterminate" structure is loaded by strong lateral loads and some joints develop plastic hinges, there is enough redundancy in the system so that other joints maintain their integrity. In this way, recentering of the structures is achieved to some extent and stability is ensured. The second concept, known as ductility, is the ability of the structure to maintain sufficient strength at large deformations. In this way, even in the event of excessive lateral loads that may convert all joints to plastic hinges, all modern seismic codes demand that these hinges shall develop sufficient ductility so that collapse is prevented; however, in this case the structure may experience appreciable permanent displacements. The third concept

*Corresponding author, Professor, E-mail: nmakris@upatras.gr

that dominates modern structural engineering is that of positive stiffnesses. When a structure behaves elastically, forces and deformations are proportional. When yielding is reached the forces are no longer proportional to the deformations; however, in most cases the stiffnesses at any instant of the deformation history of the structure remain positive—that is if some force is needed to keep the structure away from equilibrium at some displacement; then, a smaller force is needed to keep the structure away from equilibrium at a larger displacement. Fig. 1 (left) illustrates the deformation pattern of a moment-resisting, fixed-base frame when subjected to a lateral load capable to induce yielding at the joints. The force-deformation curve ($P-u$) is nonlinear; nevertheless, the lateral stiffness of the system remains positive at all times.

Fig. 1 (right) illustrates the deformation pattern of a free-standing rocking frame (two free-standing rigid columns capped with a freely supported rigid beam) when subjected to a lateral load capable to induce uplifting of the columns. The force-displacement relationship ($P-u$) of the rocking frame shown at the bottom of Fig. 1 (right) indicates that the articulated system has infinite stiffness until uplift is induced and once the four-hinge frame is set into rocking motion, its restoring force decreases monotonically, reaching zero when the rotation of the column $\theta=a=\arctan(b/h)$. Accordingly, the free-standing rocking frame shown in Fig. 1 (right) is a four-hinge mechanism that exhibits negative lateral stiffness.

Fig. 1 indicates that while most modern structural engineers are trained to design statically indeterminate structures that exhibit positive stiffnesses and hopefully sufficient ductility (Fig. 1 left); ancient builders were designing entirely different structural systems—that is articulated

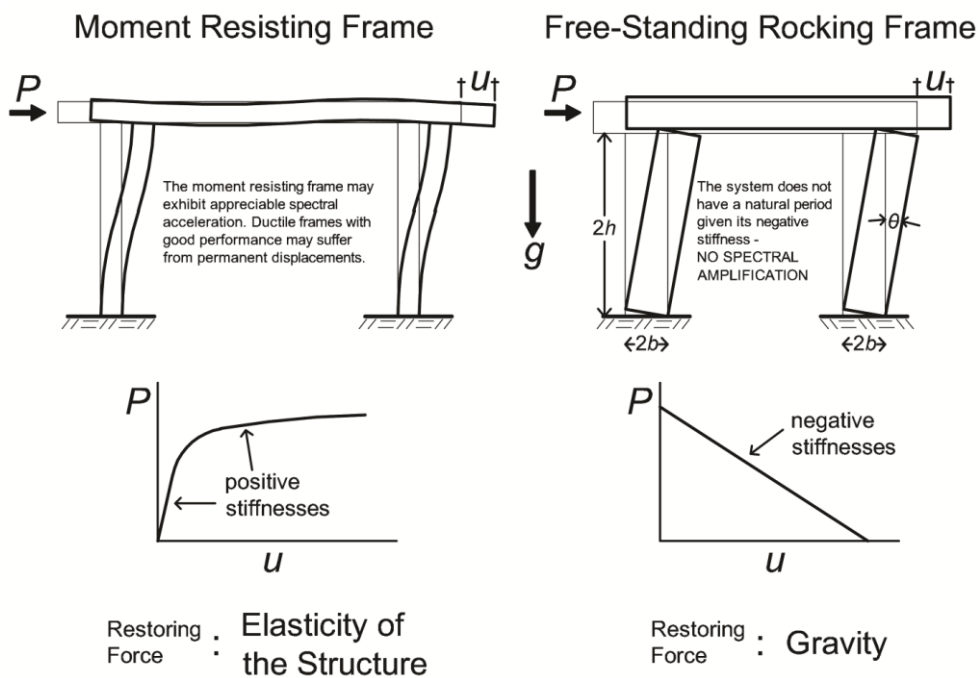


Fig. 1 The fundamental difference in the behavior of a traditional moment-resisting frame (left) and a rocking frame with free-standing columns which are allowed to rock (right)



Fig. 2 View of the Temple of Aphaia in Aegina, Greece. Its monolithic, free-standing columns support massive epistyles and the frieze atop, and the entire rocking frame remains standing for more than 2500 years in a region with high seismicity

mechanisms that exhibit negative stiffnesses and low damping (Fig. 1 right). What is remarkable about these “unconventional” articulated structures is that they have endured the test of time by surviving several strong seismic motions during their 2.5 millennia life. For instance, Fig. 2 shows the entrance view of the late archaic Temple of Aphaia in the island of Aegina nearby Athens, Greece. Dates ranging from 510 BC to 470 BC have been proposed for this temple. All but three of the 32 outer columns of the temple are monolithic and they have been supporting for 2.5 millennia the front and back epistyles together with the heavy frieze (triglyph and metope) atop.

The unparalleled seismic performance of the rocking frames shown in Fig. 2 is due to the very reason that they are articulated mechanisms. In this way: (a) given their negative stiffnesses they are not subject to any resonance, (b) recentering (elimination of any permanent displacement) is achieved unconditionally with gravity; and (c) the rocking frames, while slender and emblematic, they are large in size to the extent that their rotational inertia, when mobilized, is enough to resist the 2500 years seismic hazard.

Analytical studies on the seismic response of slender, free-standing blocks have been presented as early as in 1885 by Milne (1885) in an effort to estimate levels of ground shaking. His reasoning is entirely within the context of an equivalent static analysis and by taking moment equilibrium about the imminent pivoting point, he concludes that when the ground acceleration, \ddot{u}_g ,

exceeds the value of $g \cdot (\text{width}/\text{height})$, the block overturns. Four decades after Milne's work, Kirkpatrick (1927) published a remarkable paper on the seismic stability of rocking columns. His work brings forward the two key quantities other than the peak ground acceleration that are responsible for the stability of a slender, free-standing column: (a) the size of the column which enters the equations via the moment of inertia; and (b) the duration of the period of the excitation. Kirkpatrick (1927) after correctly deriving the minimum acceleration amplitude of a harmonic excitation that is needed to overturn a free-standing column with a given size and slenderness, proceeds by presenting the first minimum-acceleration overturning spectrum (Fig. 6 of Kirkpatrick 1927 paper) and shows that as the period of the excitation decreases, a larger acceleration is needed to overturn a free-standing column. While P. Kirkpatrick worked in Hawaii, it appears that his contributions were not known in Japan. Nevertheless, in the late 1940's Ikegami and Kishinouye published two important papers, one following the December 21, 1946 Nankai Earthquake (Ikegami and Kishinouye 1947) and the other following the December 26, 1949 Imaichi Earthquake (Ikegami and Kishinouye 1950). These two papers come to confirm Kirkpatrick's theoretical findings on the rocking response of free-standing columns; since they indicate that the static threshold, $g \cdot (\text{width}/\text{height})$, is too low and is not able to explain the observed stable response of more slender; yet, larger tombstones. In their own words Ikegami and Kishinouye (1950) write "*In our field investigations, we often met with cases where gravestones had not overturned because of their large dimensions in spite of the small value of the ratio between width and height*".

About a decade later Muto et al. (1960) build upon the work of Ikegami and Kishinouye (1947, 1950) and show explicitly that the dynamic response of a rocking column is governed by a negative stiffness; therefore, its free-vibration response is not harmonic; rather it is described by hyperbolic sines and cosines.

The pioneering work of Kirkpatrick (1927) in association with the systematic work conducted in Japan on rocking and overturning during the first-half of the 20th century matured the knowledge on this subject to the extent that Housner (1963) after introducing the concept of pulse-excitations elucidated a size-frequency scale effect that explained why (a) the larger of two geometrically similar blocks can survive the excitation that will topple the smaller block and (b) out of two same acceleration amplitude pulses, the one with longer duration is more capable to induce overturning. While the exact dynamic rocking response of the free-standing slender column turns out to be rather complex, the following section offers a qualitative explanation of the size-frequency scale effect initially identified by Kirkpatrick (1927) and made popular to the earthquake engineering community by Housner (1963).

2. A Notable Limitation of the Equivalent Static Lateral Force Analysis

2.1 Seismic Resistance of Free-Standing Columns under "Equivalent Static" Lateral Loads

Consider a free-standing rigid column with size $R = \sqrt{b^2 + h^2}$ and slenderness $b/h = \tan\alpha$ as shown in Fig. 3 (left). Let us first assume that the base of the column is moving (say to the left) with a "slowly" increasing acceleration, \ddot{u}_g (say a very long-duration acceleration pulse which allows for an equivalent static analysis). Uplift of the block (hinge formation) happens when the seismic demand (overturning moment) = $m\ddot{u}_g h$ reaches the seismic resistance (recentering moment)

$= mgb$. When uplifting is imminent, “static” moment equilibrium of the block about the pivoting point O gives

$$\underbrace{m\ddot{u}_g h}_{\text{demand}} = \underbrace{mgb}_{\text{resistance}} \quad \text{or} \quad \underbrace{\ddot{u}_g}_{\text{demand}} = g \frac{b}{h} = \underbrace{g \tan \alpha}_{\text{resistance}} \quad (1)$$

Eq. (1), also known as West’s formula (Milne 1885, Kirkpatrick 1927), shows that the block $\langle b, h \rangle$ will uplift when $\ddot{u}_g \geq g \tan \alpha$. Now, given that this is a “quasistatic” lateral inertial loading, the inertia moment due to the nearly zero rotational accelerations of the blocks is negligible ($\ddot{\theta}(t) = 0$). Upon uplift has occurred, the rocking block experiences a positive rotation, $\theta(t)$; therefore, the seismic demand is $m\ddot{u}_g R \cos(\alpha - \theta(t))$; while the seismic resistance is merely $mgR \sin(\alpha - \theta(t))$ since $\ddot{\theta}(t) = 0$. For $\theta > 0$, the resistance of the rocking block upon uplifting under quasistatic lateral loading is $\tan(\alpha - \theta(t))$ which is smaller than $\tan \alpha$. Accordingly; once the block uplifts, it will also overturn. From this analysis one concludes that under quasistatic lateral loading the stability of a free-standing column depends solely on its slenderness ($g \tan \alpha$) and is independent to the size ($R = \sqrt{b^2 + h^2}$).

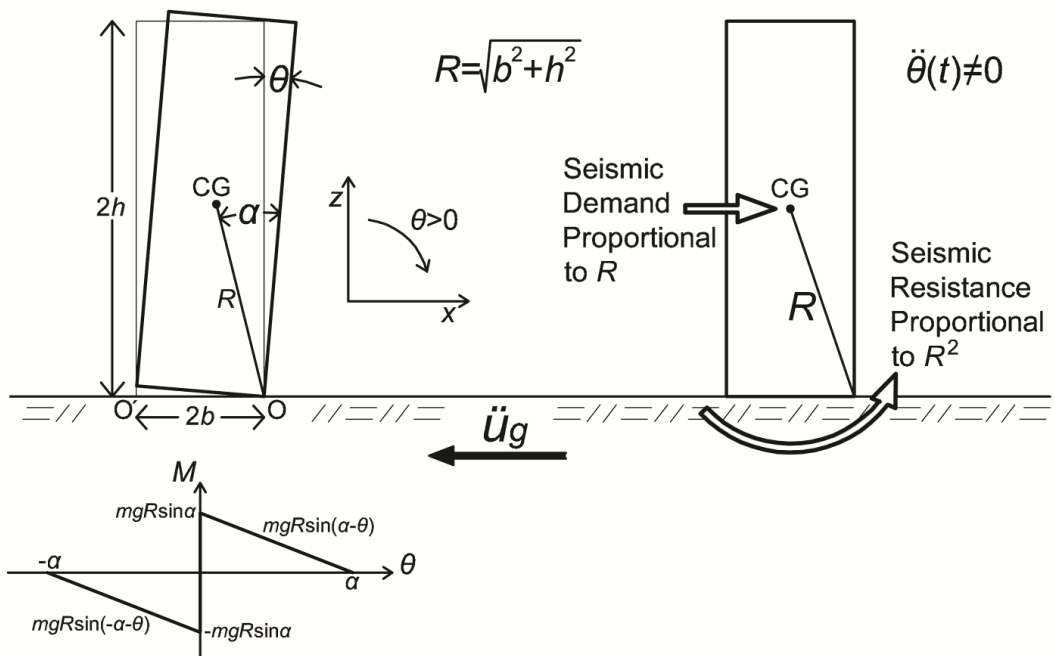


Fig. 3 Left: Geometric characteristics of a free-standing rocking column together with its moment rotation diagram. Right: During earthquake shaking which sets the column in rocking motion ($\ddot{\theta}(t) \neq 0$) the seismic resistance is proportional to R^2 ; while, the seismic demand is proportional to R . Consequently, when a free-standing column is sufficiently large it can survive large horizontal accelerations even if it is very slender

2.2 Seismic Resistance of Free-Standing Columns Subjected to Dynamic Loads

In reality, earthquake shaking, \ddot{u}_g , is not a quasistatic loading and upon uplifting has occurred the block will experience a finite rotational acceleration ($\ddot{\theta}(t) \neq 0$). In this case, dynamic moment equilibrium gives

$$\underbrace{-m\ddot{u}_g(t)R\cos[\alpha - \theta(t)]}_{\text{seismic demand}} = \underbrace{I_o\ddot{\theta}(t) + mgR\sin[\alpha - \theta(t)]}_{\text{seismic resistance}} \quad \theta > 0 \quad (2)$$

where I_o is the rotational moment of inertia of the column about the pivot point at the base—a quantity that is proportional to the square of the size of the column R . As an example for rectangular columns, $I_o = \frac{4}{3}mR^2$, and Eq. (2) simplifies to

$$\underbrace{-\ddot{u}_g(t)R\cos[\alpha - \theta(t)]}_{\text{seismic demand}} = \underbrace{\frac{4}{3}R^2\ddot{\theta}(t) + gR\sin[\alpha - \theta(t)]}_{\text{seismic resistance}} \quad \theta > 0 \quad (3)$$

Eq. (3) indicates that when a slender free-standing column is set into rocking motion the seismic demand (overturning seismic moment) is proportional to R (first power of the size); whereas, the seismic resistance (opposition to rocking) is proportional to R^2 (second power of the size). Consequently, Eq. (3) dictates that regardless how slender a column is (small α) and how intense the ground shaking, \ddot{u}_g , is (seismic demand), when a rotating column ($\ddot{\theta}(t) = \text{finite}$) is large enough, the second power of R in the right-hand-side (seismic resistance) can always ensure stability. Simply stated, Housner's (1963) size effect is merely a reminder that a quadratic term eventually dominates over a linear term regardless the values of their individual coefficients.

Fig. 3 (right) shows schematically the relations with the size R of the seismic demand (linear relation) and the seismic resistance (quadratic relation). From its very conception the “equivalent static lateral force analysis” is not meant to deal with any rotational acceleration term; therefore, its notable failure to capture the seismic stability (resistance) of tall free-standing structures. Simply stated, ancient builders were designing structures that their seismic resistance originates primarily from the mobilization of their rotational inertia—a truly dynamic design. It is worth emphasizing that slender rocking structures have low-to-moderate strength (uplifting initiates when $\ddot{u}_g > g(b/h) = gtan\alpha$), negative stiffness; whereas, damping during rocking happens only at the instant of impact; therefore, the ductility of these systems is zero. Table 1 compares the basic design concepts together with the main response-controlling quantities that are associated with: (a) the traditional earthquake resistant (capacity) design; (b) seismic isolation; and (c) rocking isolation. It is worth noting that the ancient temples as the one shown in Fig. 2 were designed by following a truly dynamic design which merely takes full advantage of the large rotational inertia of the structural members; whereas, in modern times the prevailing design philosophy is deeply rooted to static concepts such as strength and ductility; while it neglects entirely the ample seismic resistance that may originate from the mobilization of the rotational inertia of the structure (or its individual members). Perhaps, the only exception to this static design philosophy is the implementation of concave sliding bearings in seismic isolated structures where the restoring force is a component of the weight of the structure.

It is worth noting that during the last decade there has been a series of publications which aim to direct the attention of engineers to the unique advantages associated with allowing structures to uplift. The underlying concept in this class of publications is the intentional generation of uplifting mechanisms in traditional moment resisting frames (Ajrab et al. 2004, Harden et al. 2006, Kawashima et al. 2007, Gajan and Kutter 2008, Anastasopoulos et al. 2010, Hung et al. 2011, Deng et al. 2012, Gelagoti et al. 2012, among others) either at the bottom of shear walls or even at the foundation level by allowing appreciable rotations of the footings due to eccentric loading. In this way, the seismic resistance of these “hybrid” structural systems originates primarily from the intentional creation of a lower failure mechanism which once mobilized it reduces the seismic demand on other critical locations of the structure; while, rocking motion in the way that is illustrated in Fig. 3 happens only to some individual members of the overall moment-resisting yielding frame. Consequently, in this class of hybrid systems the development of rotational accelerations of the individual rocking members is somehow suppressed since their motion needs to be compatible with the lateral motion of the overall yielding frame. Accordingly, the seismic resistance of these yielding frames is “in-between” that of a traditional moment-resisting yielding frame and that of a rocking frame. In most cases the ductile behavior of the overall moment-resisting yielding frame dominates the system behavior and in this case a “capacity” design approach may be applicable (Gajan et al. 2008).

3. Aim of this Work

Despite the ample dynamic stability (seismic resistance) of large, free-standing structures as shown qualitatively in Fig. 3 (right) and quantitatively later in this paper with the overturning spectra, most modern tall bridges (with tall slender piers which if they were free-standing they could engage into stable rocking motion and mobilize their high rotational inertia) are protected from the seismic action via base-shear isolation, after designing massive pile foundations to prevent uplifting, rather than from (the most natural) rocking isolation. Part of the motivation of this paper is to bring forward the three unique advantages of rocking isolation: (a) that regardless its slenderness (aspect ratio) and the intensity of the ground acceleration, a free-standing rocking frame remains stable when is sufficiently large; (b) that given the inherent negative stiffness, a rocking frame neither amplifies nor resonates from any frequency content of the input ground motion; and (c) that recentering (elimination of any permanent displacement) is achieved unconditionally through gravity—a major asset that is always available for free. Accordingly, the aim of this work is not to present an exhaustive review on past studies that investigated various aspects of the rocking response and stability of free-standing blocks and rigid body assemblies (e.g. Allen et al. 1986, Psycharis 1990, Spanos et al. 2001, Konstantinidis and Makris 2005, 2010, Palmeri and Makris 2008, Kounadis et al. 2012, among others and references reported therein). Its aim is rather to offer the necessary theoretical background in an effort to accept and establish rocking isolation and the associated hinging mechanism which allows the mobilization of the rotational inertia of major structural members not just as limit-state mechanism; but as an operational state (seismic protection) mechanism for large slender structures.

Table 1 Basic design concepts and response-controlling quantities associated with: (a) the traditional earthquake resistant (capacity) design; (b) seismic isolation; and (c) rocking isolation

	TRADITIONAL EARTHQUAKE RESISTANCE DESIGN	SEISMIC ISOLATION	ROCKING ISOLATION
	• Moment Resisting Frames		
Strength	Moderate to Appreciable $\ddot{u}_g^y = \frac{Q}{m} = 0.10g-0.25g$	Low $\ddot{u}_g^y = \frac{Q}{m} = 0.03g-0.09g$	Moderate $\ddot{u}_g^{up} = g \frac{b}{h} = g \tan a$
Stiffness	Positive and Variable due to Yielding	Positive, Low and Constant	Negative, Constant
Ductility	Appreciable $\mu=3-6$	Very Large/Immaterial* LRB [†] : $\mu=10-30$ CSB [‡] : $\mu=1000-3000$	Zero
Damping	Moderate	Moderate to High	Low (only during impact)
Seismic Resistance Originates from:	Appreciable Strength and Ductility	Low Strength and Low Stiffness in association with the capability to accommodate Large Displacements	Low to Moderate Strength and Appreciable Rotational Inertia
Equivalent Static Lateral Force Analysis is Applicable?	YES	YES	NO
Design Philosophy	Equivalent Static	Equivalent Static	Dynamic

*Makris and Vassiliou (2011)

[†]LRB=Lead Rubber Bearings

[‡]CSB=Concave Sliding Bearings

4. Equation of Motion of the Free-Standing Rocking Block

For negative rotations ($\theta(t)<0$), the equation of motion of a rocking block is

$$-m\ddot{u}_g(t)R\cos[-\alpha - \theta(t)] = I_o\ddot{\theta}(t) + mgR\sin[-\alpha - \theta(t)] \quad \theta < 0 \quad (4)$$

Eqs. (2) and (4) are well known in the literature (Yim et al. 1980, Makris and Roussos 2000, Zhang and Makris 2001 and references reported therein) and are valid for arbitrary values of the slenderness angle $\alpha=\arctan(b/h)$. Eqs. (2) and (4) can be expressed in the compact form

$$\ddot{\theta}(t) = -p^2 \left\{ \sin[\alpha \operatorname{sgn}[\theta(t)] - \theta(t)] + \frac{\ddot{u}_g}{g} \cos[\alpha \operatorname{sgn}[\theta(t)] - \theta(t)] \right\} \quad (5)$$

In Eq. (5), the quantity $p = \sqrt{mRg/I_o}$ is the frequency parameter of the block and is an expression of its size. For rectangular blocks $p = \sqrt{3g/(4R)}$.

Fig. 3 (left) shows the moment–rotation relationship during the rocking motion of a free-standing block. The system has infinite stiffness until the magnitude of the applied moment reaches the value $mgRsina$, and once the block is rocking, its restoring force decreases monotonically, reaching zero when $\theta = \alpha$. This negative stiffness, which is inherent in rocking systems, is most attractive in earthquake engineering in terms of keeping base shears and moments low (Makris and Konstantinidis 2003), provided that the rocking block remains stable, thus the need for a formulae that will offer a safe design value for its slenderness.

During the oscillatory rocking motion, the moment–rotation curve follows the curve shown in Fig. 3 without enclosing any area. Energy is lost only during impact, when the angle of rotation reverses. The ratio of kinetic energy after and before the impact is

$$r = \frac{\dot{\theta}_2^2}{\dot{\theta}_1^2} \quad (6)$$

which means that the angular velocity after the impact is only \sqrt{r} times the velocity before the impact.

Conservation of angular momentum just before and right after the impact gives (Housner 1963):

$$\sqrt{r} = 1 - \frac{3}{2} \sin^2 \alpha \quad (7)$$

The value of the coefficient of restitution given by (7) is the maximum value of \sqrt{r} , under which a block with slenderness α will undergo rocking motion. Consequently, in order to observe rocking motion, the impact has to be inelastic. The less slender a block is (larger α), the more plastic the impact is, and for the value of $\alpha = \sin^{-1} \sqrt{2/3} = 54.73^\circ$, the impact is perfectly plastic. During the rocking motion of slender blocks, if additional energy is lost due to the inelastic behavior at the instant of impact, the value of the true coefficient of restitution r will be less than the one computed from Eq. (7).

Following Housner's seminal paper, a number of studies have been presented to address the complex dynamics of one of the simplest man-made structures—the free-standing rigid column. Yim et al. (1980) conducted numerical studies by adopting a probabilistic approach; Aslam et al. (1980) confirmed with experimental studies that the rocking response of rigid blocks is sensitive to system parameters, whereas Psycharis and Jennings (1983) examined the uplift of rigid bodies supported on viscoelastic foundation. Subsequent studies by Spanos and Koh (1984) investigated the rocking response due to harmonic steady-state loading and identified 'safe' and 'unsafe' regions together with the fundamental and subharmonic modes of the system. Their study was extended by Hogan (1989, 1990) who further elucidated the mathematical structure of the problem by introducing the concepts of orbital stability and Poincaré sections. The steady-state rocking response of rigid blocks was also studied analytically and experimentally by Tso and Wong (1989a,b). Their experimental work provided valuable support to theoretical findings.

Depending on the level and form of the ground acceleration, in association with the interface conditions at the base, a free-standing rigid block may translate with the ground, slide, rock, or slide-rock. Analytical and numerical studies on the possible motions of a rigid body were

presented by Ishiyama (1982) and Sinopoli (1989). These studies were followed by Scalia and Sumbatyan (1996) and Shenton (1996), who independently indicated that, in addition to pure sliding and pure rocking, there is a slide-rock mode and its manifestation depends not only on the width-to-height ratio and the static friction coefficient but also on the magnitude of the base acceleration.

5. Time Scale and Length Scale of Pulse-Like Ground Motions

The relative simple form, yet destructive potential of near-source ground motions has motivated the development of various closed-form expressions that approximate their leading kinematic characteristics. The early work of Veletsos et al. (1965) and Bertero et al. (1978) was followed by the papers of Hall et al. (1995), Makris (1997), Makris and Chang (2000), Alavi and Krawinkler (2001), and more recently by Mavroeidis and Papageorgiou (2003), Baker (2007) and Vassiliou and Makris (2011). Some of the proposed pulses are physically realizable motions with zero final ground velocity and finite accelerations, whereas some other idealizations violate one or both of the above requirements. Physically realizable pulses can adequately describe the impulsive character of near-fault ground motions both qualitatively and quantitatively. The input parameters of the model have an unambiguous physical meaning. The minimum number of parameters is two, which are either the acceleration amplitude, a_p , and duration, T_p , or the velocity amplitude, v_p , and duration, T_p (Makris (1997), Makris and Chang (2000)). The more sophisticated model of Mavroeidis and Papageorgiou (2003) involves four parameters, which are the pulse period, the pulse amplitude, together with the number and phase of half cycles, and was found to describe a large set of velocity pulses generated due to forward directivity or permanent translation effect. Recently, Vassiliou and Makris (2011) used the Mavroeidis and Papageorgiou (2003) model in association with wavelet analysis to develop a mathematically formal and objective procedure to extract the time scale and length scale of strong ground motions.

The current established methodologies for estimating the pulse characteristics of a wide class of records are of unique value since the product, $a_p T_p^2 = L_p$, is a characteristic length scale of the ground excitation and is a measure of the persistence of the most energetic pulse to generate inelastic deformations (Makris and Black 2004a). It is emphasized that the persistence of the pulse is a different characteristic than the strength of the pulse, which is measured with the peak pulse acceleration. The reader may recall that among two pulses with different acceleration amplitude (say $a_{p1} > a_{p2}$) and different pulse duration (say $T_{p1} < T_{p2}$), the inelastic deformation does not scale with the peak pulse acceleration (most intense pulse) but with the stronger length scale (larger $a_p T_p^2$ = most persistent pulse), Makris and Black (2004a,b), Karavassilis et al. (2010).

The heavy line in Fig. 4 (top) that approximates the long-period acceleration pulse of the NS component of the 1992 Erzincan, Turkey, record is a scaled expression of the second derivative of the Gaussian distribution, $e^{-t^2/2}$, known in the seismology literature as the symmetric Ricker wavelet (Ricker 1943, 1944) and widely referred to as the “Mexican Hat” wavelet (Addison 2002)

$$\ddot{u}_g(t) = a_p \left(1 - \frac{2\pi^2 t^2}{T_p^2} \right) e^{-\frac{1}{2} \frac{2\pi^2 t^2}{T_p^2}} \quad (8)$$

The value of $T_p = 2\pi/\omega_p$ is the period that maximizes the Fourier spectrum of the Symmetric Ricker Wavelet. Similarly, the heavy line in Fig. 4 (center) which approximates the long-period acceleration pulse of the Pacoima Dam motion recorded during the February 9, 1971, San Fernando, California, earthquake is a scaled expression of the third derivative of the Gaussian distribution $e^{-t^2/2}$

$$\ddot{u}_g(t) = \frac{a_p}{\beta} \left(\frac{4\pi^2 t^2}{3T_p^2} - 3 \right) \frac{2\pi t}{\sqrt{3}T_p} e^{-\frac{1}{2} \frac{4\pi^2 t^2}{3T_p^2}} \quad (9)$$

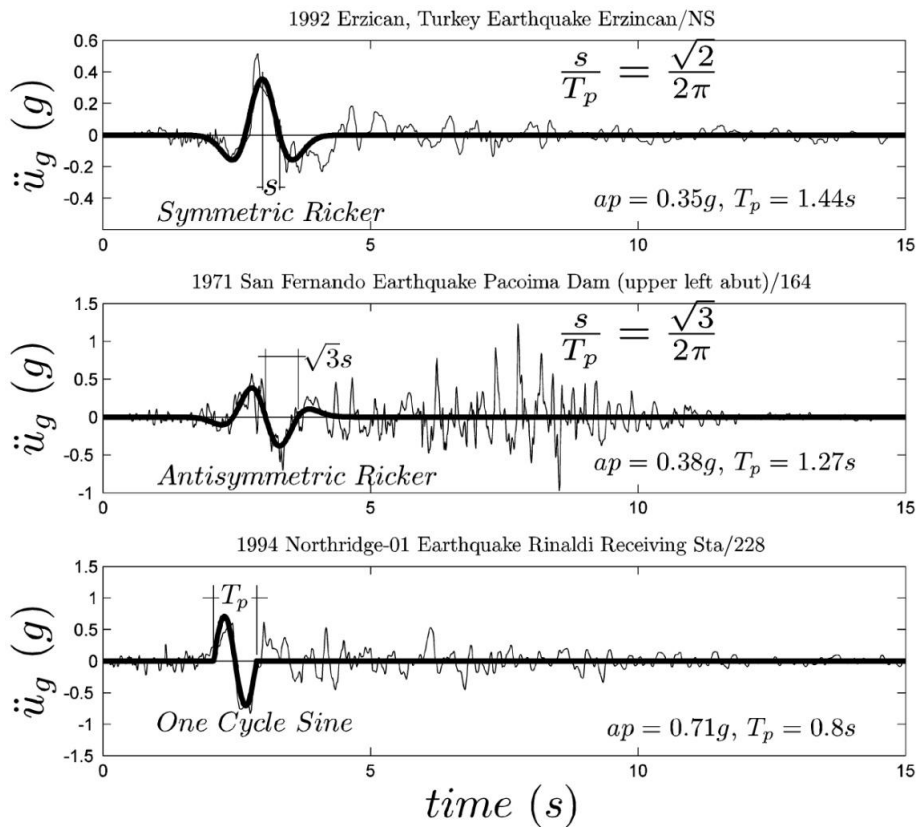


Fig. 4 Acceleration time histories recorded during the (top) 1992 Erzincan, Turkey, earthquake together with a symmetric Ricker wavelet; (center) 1971 San Fernando earthquake—fault normal component of the Pacoima Dam record together with an antisymmetric Ricker wavelet; and (bottom) 1994 Northridge earthquake—228 Rinaldi station together with a one-cycle sine pulse

in which β is a factor equal to 1.38 that enforces the above function to have a maximum= a_p . The choice of the specific functional expression to approximate the main pulse of pulse-type ground motions has limited significance in this work. In the past, simple trigonometric pulses have been proposed by the author and his coworkers (Makris 1997, Makris and Chang 2000, Makris and Black 2004a,b) to extract the time scale and length scale of pulse-type ground motions. For instance, the heavy line in Fig. 4 (bottom) which approximates the strong coherent acceleration pulse of the 228 component at the Rinaldi receiving station of the 1994 Northridge earthquake is a one-sine acceleration pulse

$$\ddot{u}_g(t) = a_p \sin(\omega_p t), \quad 0 < t < T_p \quad (10)$$

A mathematically rigorous and easily reproducible methodology based on wavelet analysis to construct the best matching wavelet on a given record (signal) has been recently proposed by Vassiliou and Makris (2011).

6. Conditions for Initiating and Sustaining Rocking Motion

Consider the free-standing rigid block shown in Fig. 3 with slenderness α , which can rock about the centers of rotation O and O' when it is set to rocking. Depending on the level and form of the ground acceleration, a free-standing block may translate with the ground, slide, rock, or

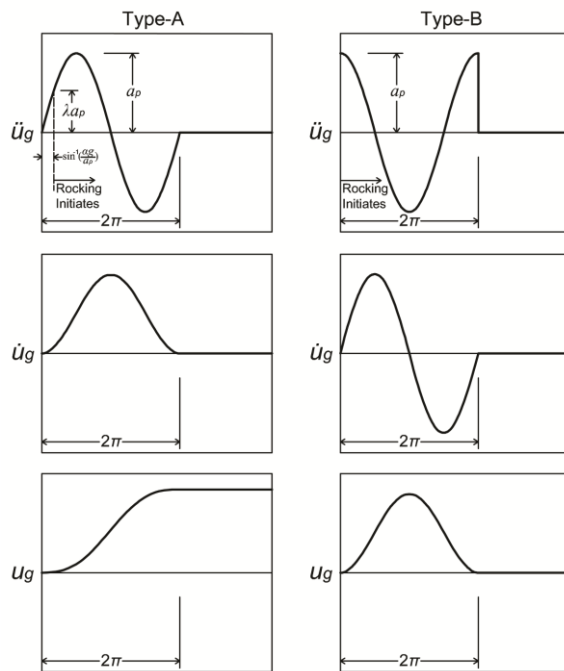


Fig. 5 Acceleration, velocity, and displacement histories of one-sine pulse (left) and one-cosine pulse (right)

slide rock. Prior to 1996, the mode of rigid-body motion that prevailed has been determined by comparing the available static friction to the width-to-height ratio of the block, irrespective of the magnitude of the horizontal ground acceleration. At about the same time, Scalia and Sumbatyan (1996) and, independently, Shenton (1996) indicated that, in addition to pure sliding and pure rocking, there is a slide-rock mode and its manifestation depends not only on the width-to-height ratio and the static friction coefficient but also on the magnitude of the base acceleration.

Physically realizable cycloidal pulses like those introduced in the previous section have displacement histories that are continuous and differentiable signals that build up gradually from zero. Their corresponding acceleration histories might be zero at the time origin or exhibit a finite value that can be as large as their maximum amplitude. Fig. 5 plots the acceleration, velocity, and displacement histories of a one-sine pulse (left) and one-cosine pulse (right). In the case of the one-sine pulse, the ground acceleration is zero at the initiation of motion and builds up gradually. In contrast, in the case of a one-cosine pulse, the ground acceleration assumes its maximum value at the initiation of motion. Under other cycloidal pulses such as Type- C_n pulses (Makris and Roussos 1998, 2000), the ground acceleration is finite at the initiation of motion; nevertheless, it assumes a value that is smaller than its maximum amplitude a_p . With reference to Fig. 3 and assuming that the coefficient of friction $\mu > (b/h) = \tan\alpha$, static equilibrium yields that the minimum horizontal acceleration that is needed to initiate rocking is $\ddot{u}_{g,min} = g\tan\alpha$ (see Eq. (1)).

6.1 Condition for Initiating Rocking Motion

Consider a cycloidal pulse with acceleration amplitude $a_p > g\tan\alpha$ and let λa_p be the value of the ground acceleration when a block with slenderness α is about to enter rocking motion. Depending on the type of pulse, λ assumes different values; however, it is bounded by

$$\frac{g\tan\alpha}{a_p} < \lambda \leq 1 \quad (11)$$

Fig. 6 shows the free-body diagram of a free-standing block that is about to enter rocking motion due to a positive ground acceleration. With the system of axis shown, a positive acceleration will induce an initial negative rotation ($\theta < 0$). Adopting the notation introduced by Shenton (1996), let $f_x > 0$ and $f_z > 0$ be the horizontal and vertical reactions at the tip O' of the block. Dynamic equilibrium at this instant ($\theta = 0$) gives

$$f_x(0) = m(\lambda a_p + h\ddot{\theta}(0)) \quad (12)$$

$$f_z(0) = m(g - b\ddot{\theta}(0)) \quad (13)$$

$$I_{cg}\ddot{\theta}(0) = -f_x(0)h + f_z(0)b \quad (14)$$

where I_{cg} = moment of inertia of the block about its center of gravity (for rectangular blocks $I_{cg} = mR^2/3$). Substitution of Eqs. (12) and (13) into Eq. (14) gives the value of the angular acceleration $\ddot{\theta}_0$ at the instant when rocking initiates

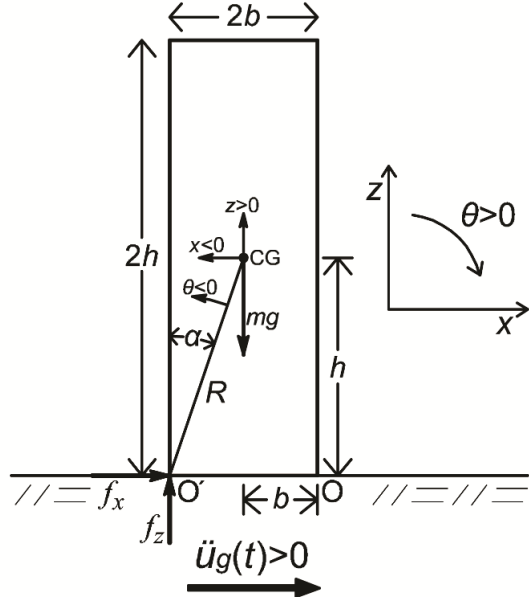


Fig. 6 Free-body diagram of rigid block at the instant that it enters rocking motion

$$\ddot{\theta}(0) = \ddot{\theta}_o = -p^2 \sin \alpha \left(\frac{\lambda a_p}{g \tan \alpha} - 1 \right) \quad (15)$$

in which $p = \sqrt{3g/(4R)}$ = frequency parameter of the block (rad/s); whereas $R = \sqrt{b^2 + h^2}$ = half-diameter of the block—a measure of its size. To avoid sliding at this instant ($t = 0$)

$$\frac{f_x(0)}{f_z(0)} \leq \mu \quad (16)$$

and substitution of the value computed by Eq. (15) into Eqs. (12) and (13) gives the condition for a block to enter the rocking motion without sliding

$$\frac{\lambda a_p - \frac{3}{4} g \cos \alpha \sin \alpha \left(\lambda \frac{a_p}{g \tan \alpha} - 1 \right)}{g + \frac{3}{4} g \sin^2 \alpha \left(\lambda \frac{a_p}{g \tan \alpha} - 1 \right)} \leq \mu \quad (17)$$

Eq. (17), initially presented by Shenton (1996) and subsequently by Pompei et al. (1998), indicates that, under some excitation pulses with amplitude a_p , the condition for a block to enter rocking motion without sliding depends on the value of a_p . However, this is true only for pulses that have a finite acceleration at the initiation of motion. For pulses in which acceleration history builds up gradually (such as a one-sine pulse), the value of λa_p at the initiation of rocking is equal to $g \tan \alpha$ and Eq. (17) reduces to

$$\tan\alpha = \frac{b}{h} \leq \mu \quad (18)$$

which is the traditional expression that one derives from static analysis.

6.2 Condition for Sustaining Rocking Motion

Once the block enters rocking motion, the horizontal reaction $f_x(t)$ and vertical reaction $f_z(t)$ fluctuates with time. Consequently, to avoid sliding during the entire duration of the rocking motion

$$\left| \frac{f_x(t)}{f_z(t)} \right| < \mu \quad \text{at all times} \quad (19)$$

Dynamic equilibrium in the horizontal and vertical directions gives

$$f_x(t) = m(\ddot{u}_g(t) + \ddot{x}(t)) \quad (20)$$

$$f_z(t) = m(g + \ddot{z}(t)) \quad (21)$$

where $x(t)$ and $z(t)$ = horizontal and vertical displacements of the center of mass of the block. The kinematics of the rocking motion yields that (Pompei et al. 1998, Zhang and Makris 2001)

$$\ddot{x}(t) = R\ddot{\theta}(t)\cos[\alpha \operatorname{sgn}[\theta(t)] - \theta(t)] + R\dot{\theta}(t)^2 \sin[\alpha \operatorname{sgn}[\theta(t)] - \theta(t)] \quad (22)$$

$$\ddot{z}(t) = R\ddot{\theta}(t)\sin[\alpha \operatorname{sgn}[\theta(t)] - \theta(t)] - R\dot{\theta}(t)^2 \cos[\alpha \operatorname{sgn}[\theta(t)] - \theta(t)] \quad (23)$$

where $\dot{\theta}(t)$ = angular velocity of the block; and $\ddot{\theta}(t)$ = angular acceleration of the block that is given by Eq. (5). The substitution of Eqs. (20) and (21) into Eq. (19) in association with Eqs. (5), (22), and (23) gives that the condition needed to avoid sliding during the entire rocking motion is (Zhang and Makris 2001)

$$\left| \frac{f_x(t)}{f_z(t)} \right| = \left| \frac{\frac{\ddot{u}_g}{g}(5 - 3\cos 2[\alpha \operatorname{sgn}[\theta] - \theta]) - 3\sin 2[\alpha \operatorname{sgn}[\theta] - \theta] + 6\frac{\dot{\theta}^2}{p^2} \sin[\alpha \operatorname{sgn}[\theta] - \theta]}{5 - 3\frac{\ddot{u}_g}{g} \sin 2[\alpha \operatorname{sgn}[\theta] - \theta] + 3\cos 2[\alpha \operatorname{sgn}[\theta] - \theta] - 6\frac{\dot{\theta}^2}{p^2} \cos[\alpha \operatorname{sgn}[\theta] - \theta]} \right| < \mu \quad (24)$$

Eq. (24) is central in accepting and establishing the concept of rocking isolation since the designer can easily verify whether a free-standing structure will only rock without sliding during the entire duration of the ground shaking. An enhanced form of Eq. (24) which also includes the effect of vertical acceleration has been presented by Taniguchi (2002) who concludes that there are cases where the contribution of the vertical acceleration needs to be considered to ensure that rocking motion is sustained.

7. Minimum Overturning Acceleration Spectra: Self-Similar Response

In his effort to address the dynamics of the rocking block a half a century ago, Housner (1963) uses as ground excitations simple mathematical pulses. In that study, the base acceleration was represented with a rectangular or a half-sine pulse $\ddot{u}_g(t)=a_p \sin(\omega_p t + \psi)$, $-\psi/\omega_p < t < (\pi - \psi)/\omega_p$ and expressions were derived for the minimum acceleration of a pulse with a given duration that is needed to overturn a free-standing block with a given size and slenderness. Thus, the first minimum overturning spectra for pulse excitation were published.

7.1 Conditions to Reach the Verge of Overturning

When calculated his overturning spectra, George Housner postulated that the condition for overturning is that the angle of rotation, θ , is equal to the block slenderness α at time $t=(\pi - \psi)/\omega_p$ which is the time at which the half-sine expires. Based on this forced and therefore flawed postulate, he derived a simple expression that provides the minimum acceleration amplitude required to overturn the block.

In reality, when the excitation pulse assumes its minimum overturning acceleration amplitude the free-standing block will reach “asymptotically” the verge of overturning ($\theta(t_{ov})=\alpha$, $\dot{\theta}(t_{ov})=0$) during its free vibration regime.

The correct condition for a rocking block to reach the verge of overturning was presented for the first time by Shi et al. (1996) who stated correctly that for the minimum overturning amplitude needed to overturn the block, the kinetic energy of the block at the verge of overturning shall be zero. Accordingly, for a half-sine pulse, Shi et al. (1996) showed that the minimum overturning acceleration amplitude $a_p = g \tan \alpha / \sin \psi$ is determined from the solution of the transcendental equation

$$\frac{\omega_p}{p} \sin \psi - \cos \psi = \exp\left[-\frac{p}{\omega_p}(\pi - \psi)\right] \quad (25)$$

Eq. (25) was derived independently by Makris and Roussos (1998, 2000) who stated that when the free-standing block is excited by the minimum overturning acceleration pulse the time needed to reach the verge of overturning ($\theta(t_{ov})=\alpha$) is theoretically infinite; and therefore $\tan(pt_{ov})=1$. With these two overturning conditions ($\theta(t_{ov})=\alpha$, $\tan(pt_{ov})=1$) Makris and Roussos (1998, 2000) concluded that the minimum overturning acceleration amplitude $a_p = g \tan \alpha / \sin \psi$ is determined from the solution of the transcendental equation

$$\begin{aligned} \cos \psi \cosh\left[\frac{p}{\omega_p}(\pi - \psi)\right] - \frac{\omega_p}{p} \sin \psi \sinh\left[\frac{p}{\omega_p}(\pi - \psi)\right] + \\ \cos \psi \sinh\left[\frac{p}{\omega_p}(\pi - \psi)\right] - \frac{\omega_p}{p} \sin \psi \cosh\left[\frac{p}{\omega_p}(\pi - \psi)\right] = -1 \end{aligned} \quad (26)$$

Using the definition of the hyperbolic functions, Eq. (26) simplifies to Eq. (25) initially derived by Shi et al. (1996).

Today, the solution given by Eq. (25) or (26) has a limited design value, since a half-cycle

acceleration pulse is not a physically realizable pulse because it results to infinite ground displacements. Nevertheless, the efforts of Shi et al. (1996) and Makris and Roussos (1998, 2000) are important contributions in the development of the theory of rocking isolation since they established the correct conditions at the verge of overturning ($\theta(t_{ov}) = \alpha$, $\dot{\theta}(t_{ov}) = 0$ or alternatively $\tan(pt_{ov}) = 1$), which are central in establishing the minimum design slenderness of a free-standing structure with a given height (see Makris and Vassiliou 2012).

7.2 Overturning Spectra from Physically Realizable Pulses

Following the spectacular damage of the Olive View Hospital during the 1971 San Fernando, California earthquake, Bertero et al. 1978 directed the attention of engineers to long-duration acceleration pulses which result in unusually large monotonic velocity increments. During the subsequent 15 years, there have been a handful of publications that stressed the significance of long-duration pulses (Bertero et al. 1991, Somerville and Graves 1993); however, it was only after the 1994 Northridge, California and the 1995 Kobe Japan earthquake that researchers recognized that the use of simple mathematical pulses as ground excitations may reveal significant information on peak response quantities of various structural systems.

Given that the half sine and rectangular pulses used by Housner (1963) are not physically realizable ground motions (they result to infinite ground displacements), Makris and Roussos (1998) examined the rocking response and stability of slender blocks to physically realizable pulses such as the one-sine acceleration pulse (type-A=forward pulse) and the one-cosine pulse (type-B=forward-and-back pulse) shown in Fig. 5, together with more complex pulses where the displacement history exhibits one or more long duration cycles (type-C pulses). Using these pulses, Makris and Roussos (1998) presented for the first time minimum overturning acceleration spectra for rocking blocks by solving numerically the nonlinear equation of motion given by Eq. (5).

The 1998 Makris and Roussos report summarized seismic response and stability studies on electrical equipment with a frequency parameter $p \approx 2\text{rad/sec}$. In view of the relatively long duration of the coherent pulses that is needed to induce overturning (say $T_p > 1\text{sec}$), the range of interest in the frequency ratio, ω_p/p , for rocking stability of electrical equipment ($p \approx 2\text{rad/sec}$) is $0 \leq \omega_p/p \leq \pi$. Within this range of dimensionless frequency ($0 \leq \omega_p/p \leq \pi$), the minimum overturning acceleration spectra due to cycloidal pulses is nearly linear and Makris and Roussos (1998, 2000) proposed the approximate expression for the minimum overturning acceleration amplitude

$$\frac{a_{po}}{g \tan \alpha} = 1 + \beta \frac{\omega_p}{p} \quad (27)$$

In Eq. (27), a_{po} is the minimum overturning acceleration amplitude of the pulse and α is the slenderness angle of the block. The coefficient $\beta = 1/6$ for Type-A or Type-C_n pulses and $\beta = 1/4$ for Type-B pulses. For values of $\omega_p/p \geq \pi$, the minimum overturning acceleration spectra becomes increasingly nonlinear. Although the range of $\omega_p/p \geq \pi$ is not of interest in evaluation the rocking stability of relative small free-standing blocks (electrical transformers with $p=2$) it is of prime interest when assessing the rocking stability of larger structures (ancient free-standing columns or prefabricated bridge frames, $p < 1$) excited by shorter duration pulses.

Shortly after the publication of the Makris and Roussos (1998) report, Anooshehpoor et al. (1999) presented minimum overturning acceleration spectra due to one-sine acceleration pulse by

solving the linearized expressions of Eqs. (2) and (4). Their study was motivated from the temptation to estimate peak ground accelerations at Point Reyes, California, during the 1906 San Francisco earthquake. Their semi-analytical solution focused on the one-impact mode of overturning; without recognizing the presence of the second mode of overturning that happens without impact. This second mode of overturning (without impact) further complicates the dynamics of the response, while the transition from the first mode (with impact) to the second mode (without impact), which happens in the neighborhood of $\omega_p/p \approx 6-10$ is sensitive to the nonlinear nature of the problem (Zhang and Makris 2001).

Before examining the minimum overturning acceleration spectra with a full nonlinear analysis for values of $\omega_p/p > \pi$ —that is for large blocks or high frequency pulses, we return to Eq. (27) that was initially presented by Makris and Roussos (1998) within the context of a demand assessment (find the acceleration level capable to overturn a free-standing block with a given slenderness α and a given size p). As rocking isolation gradually emerged as an attractive seismic design concept, there was a need of sizing the width of tall free-standing columns with a given size. This need can be addressed by expressing Eq. (27) within the context of a capacity design (find the geometry of the structure that can sustain a given loading). Accordingly, Eq. (27) gives

$$\tan \alpha = \frac{a_p}{g} \left(\frac{pT_p}{\gamma + pT_p} \right) \quad (28)$$

where $T_p = 2\pi/\omega_p$ and $\gamma = 2\pi\beta$ —that is $\gamma = \pi/3$ for Type-A and Type-C_n pulses and $\gamma = \pi/2$ for a Type-B pulse. Eq. (28), which is extracted by fitting the minimum overturning acceleration spectra computed numerically by Makris and Roussos (1998) was re-discovered some 15 years later after employing basic principles of dynamics (Makris and Vassiliou 2012).

The various mathematical idealizations of coherent pulse-type ground motions as described by Eqs. (8) to (10) and shown in Figs. 4 and 5 are invariably characterized by a pulse period T_p and a pulse acceleration amplitude a_p . From Eq. (5), it results that the response of a rocking free-standing block subjected to ground acceleration pulse is a function of five variables

$$\theta(t) = f(p, \alpha, g, a_p, \omega_p) \quad (29)$$

The six variables appearing in Eq. (29), $\theta \doteq []$, $a_p \doteq [L][T]^{-2}$, $\omega_p \doteq [T]^{-1}$, $p \doteq [T]^{-1}$, $\alpha \doteq []$, $g \doteq [L][T]^{-2}$ involve only two reference dimensions: those of length [L] and time [T]. According to Vashy-Buckingham's Π -theorem (Barenblatt 1996), the number of dimensionless products with which the problem can be completely described is equal to [number of variables in Eq. (29)=6]—[number of reference dimensions=2]. Herein, we select as repeating variables the characteristics of the pulse excitation, a_p and ω_p , and in this case the four independent Π -terms are

$$\Pi_\theta = \theta \quad (30)$$

$$\Pi_\omega = \frac{\omega_p}{p} \quad (31)$$

$$\Pi_\alpha = \tan\alpha \quad (32)$$

$$\Pi_g = \frac{a_p}{g} \quad (33)$$

With the four dimensionless Π -terms established, Eq. (29) reduces to

$$\theta(t) = \varphi\left(\frac{\omega_p}{p}, \tan\alpha, \frac{a_p}{g}\right) \quad (34)$$

The rocking response of a rigid block when subjected to a horizontal base acceleration, $\ddot{u}_g(t)$ is computed by solving Eq. (5) in association with the minimum energy loss expression given by Eq. (7), which takes place at every impact. The solution of the nonlinear differential equation given by (5) is computed numerically by means of a state-space formulation. The state vector of the system shown in Fig. 3 (left) is merely

$$\mathbf{y}(t) = \begin{bmatrix} \theta(t) \\ \dot{\theta}(t) \end{bmatrix} \quad (35)$$

and the time-derivative vector $\mathbf{f}(t) = \dot{\mathbf{y}}(t)$ is

$$\dot{\mathbf{y}}(t) = \begin{bmatrix} \dot{\theta}(t) \\ -p^2[\sin[\alpha \operatorname{sgn}[\theta(t)] - \theta(t)] + \frac{\ddot{u}_g(t)}{g} \cos[\alpha \operatorname{sgn}[\theta(t)] - \theta(t)]] \end{bmatrix} \quad (36)$$

The numerical integration of Eq. (36) is performed with standard ordinary differential equations (ODE) solvers available in MATLAB, The Mathworks (2002).

Fig. 7 shows the overturning acceleration spectrum of a rigid block with slenderness $\alpha = 10^\circ$ ($b/h=1/5.67$, $\tan\alpha = 0.176$) due to a one-sine acceleration pulse (left), a symmetric Ricker wavelet (center), and an antisymmetric Ricker wavelet (right). Fig. 7 indicates that as $\Pi_\omega = \omega_p/p$ increases, the acceleration needed to overturn the object becomes appreciably larger than the one needed to uplift it. When producing the results of Figure 7, the maximum coefficient of restitution given by Eq. (7) was used.

The light gray area in all three bottom plots corresponds to stability (no overturning). The areas in black in all three plots correspond to overturning without impact. The gray areas below the black areas correspond to overturning with one impact. The gray areas above the black areas correspond to overturning with multiple impacts which do not exist in the case of one-sine acceleration pulse (left plot). Note that all three plots show that there are safe areas above the minimum overturning acceleration—a behavior that results from the strong nonlinear nature of the problem. Most important is that as the ratio $\Pi_\omega = \omega_p/p$ increases (shorter duration pulses or larger blocks), the minimum overturning acceleration needed to overturn the block increases appreciably. This size-frequency effect illustrated in Fig. 7 shows that a block with a given slenderness can survive strong shaking, provided that it is large enough.

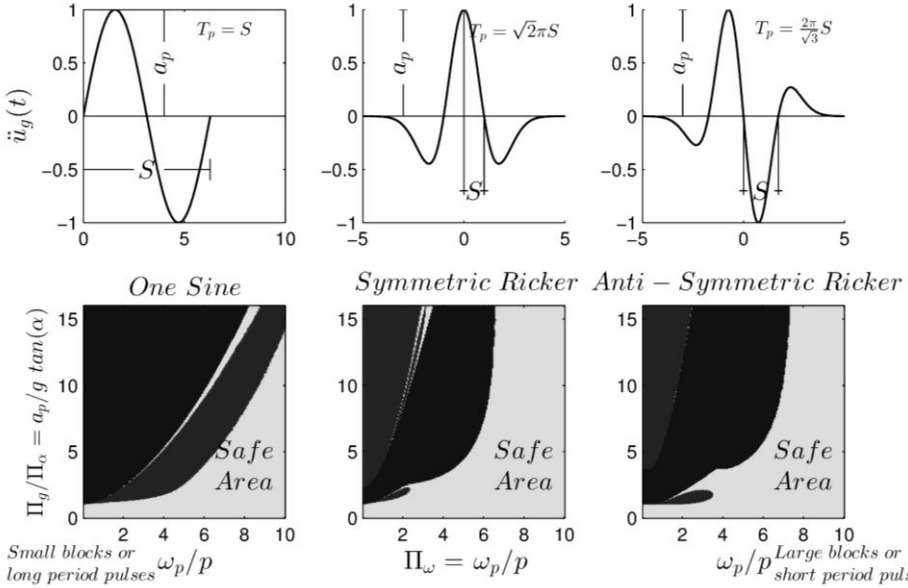


Fig. 7 Overturning acceleration spectra of a free-standing block with slenderness $\alpha = 10^\circ$, subjected to a one-sine acceleration pulse (left), a symmetric Ricker wavelet (center), and an antisymmetric Ricker wavelet (right). The light gray areas (safe areas) in all three plots correspond to stability (no overturning). The areas shaded in black in all three plots correspond to overturning without impact. The gray areas below the black areas correspond to overturning with one impact. The gray areas above the black areas correspond to overturning with multiple impacts which do not exist in the case of one-sine acceleration pulse (left plot).

8. Sizing the Slenderness (aspect ratio) of a Free-Standing Column with a Given Height to Withstand Earthquake Shaking

The main challenge in designing rocking structures in order to limit overturning moments and base shears is that the restoring moment of a rocking structure decreases as rotation increases (see Fig. 3) and eventually becomes unstable when the rotation exceeds the slenderness, α , of the free-standing structure. Accordingly, when sizing a rocking structure, it has to be slender enough to undergo rocking; while, it has to be wide enough in order to remain stable, given the seismic hazard of the area that it belongs to. Accordingly, this section summarizes the derivation of a closed-form expression presented recently by Makris and Vassiliou (2012) that offers the minimum design slenderness that is sufficient for a free-standing column with a given height to survive a pulse-like motion with known acceleration amplitude and duration.

8.1 Approach with dimensional and physical arguments

The solution to the problem addressed above can be approached with the use of the dimensionless products given by Eqs. (30)–(33) in association with the information from static

analysis—that for a long-duration (constant) acceleration pulse with amplitude a_p , the overturning acceleration is $a_p = gt \tan \alpha$ (see Eq. (1)). Accordingly, after replacing the dimensionless term $\Pi_\omega = \omega_p/p$ with pT_p , the minimum slenderness α that ensures stability of a free-standing block with size R subjected to a pulse with amplitude a_p and duration T_p is

$$\tan \alpha = \frac{a_p}{g} \varphi(pT_p), \text{ or } \Pi_\alpha = \Pi_g \varphi(\Pi_\omega) \quad (37)$$

Now, while the expression of the function $\varphi(pT_p)$ is unknown, physical arguments discussed in the introduction of this paper indicate its limits as pT_p is very small or very large.

$$\begin{aligned} \lim_{pT_p \rightarrow 0} \varphi(pT_p) &= 0 & \lim_{pT_p \rightarrow \infty} \varphi(pT_p) &= 1 \\ \text{large blocks or high - frequency pulses} & & \text{small blocks or long - period pulses} & \end{aligned} \quad (38)$$

With the two limiting values of $\varphi(pT_p)$ established, one can propose approximate expressions for the function $\varphi(pT_p)$. For instance, Eq. (28) that is back-calculated after fitting the minimum overturning acceleration spectra due to simple cycloidal pulses satisfies the limiting values offered by Eq. (38). The challenging question however is whether the mathematical form of Eq. (37) can be derived from basic principles of dynamics.

8.2 Analytical approach

In order to address this problem analytically, Makris and Vassiliou (2012) first examined what is the minimum initial angular velocity, $\dot{\theta}(0)$, that is needed to bring a free-standing block at the verge of overturning—a limit state that is defined when the diagonal of the block is vertical $\theta(t_{ov}) = \alpha$ and the angular velocity at this position is zero ($\dot{\theta}(t_{ov}) = 0$). At this limit state, for the angular velocity $\dot{\theta}(t)$ to reach asymptotically the zero-value as $\theta(t)$ tends to α , it takes theoretically an infinite amount of time; therefore, t_{ov} is in any event sufficiently larger than any finite time interval which appears in the problem at hand. In theory, the acceleration amplitude can be tuned to the extent that the block will take an infinite long time to decide whether it will re-center or overturn.

For rectangular blocks, $I_0 = (4/3)mR^2$, the minimum initial angular velocity needed to bring a rocking block $\langle \alpha, p \rangle$ at the verge of overturning is (Palmeri and Makris 2008, Makris and Vassiliou 2012)

$$\dot{\theta}(0) = \alpha p \quad (39)$$

Given the result of Eq. (39), our problem now reduces in identifying what shall be the acceleration amplitude and duration of a pulse capable of inducing an initial angular velocity $\dot{\theta}(t = T_p) = \alpha p$. It is known (Makris and Roussos 1998, 2000) that the shape of the pulse influences the exact value of the slenderness needed for the block to remain standing; nevertheless, it is also known that the rectangular pulse has the strongest overturning potential among all other physically realizable pulses (differentiable acceleration signals that produce finite ground displacement) with the same amplitude and duration. Consequently, a rectangular pulse yields conservative results,

which are attractive in design. Accordingly, we proceed by examining what is the angular velocity induced in a free-standing block excited by a rectangular pulse with acceleration amplitude a_p and duration T_p . Fig. 6 shows the free-body diagram of a free-standing block that is about to enter rocking motion due to a positive ground acceleration; while Eq. (15) gives the value of the angular acceleration $\ddot{\theta}(0)$ at the instant when rocking initiates.

Eq. (15) indicates that the free-standing column initiates its motion with a finite angular acceleration $=\ddot{\theta}(0)$. Makris and Vassiliou (2012) observed that during the duration, $0 \leq t \leq T_p$, of a rectangular pulse, the value $\ddot{\theta}(t)$ maintains a nearly constant value ($\ddot{\theta}(t) \approx \ddot{\theta}(0)$ for $0 \leq t \leq T_p$), thus the nearly linear increase in the angular velocity. Accordingly, at the expiration of the pulse, the angular velocity of the block is approximately

$$\dot{\theta}(t = T_p) = \int_0^{T_p} \ddot{\theta}(0) dt = -p^2 \sin \alpha \left(\frac{a_p}{g \tan \alpha} - 1 \right) \int_0^{T_p} dt = -p^2 \sin \alpha \left(\frac{a_p}{g \tan \alpha} - 1 \right) T_p \quad (40)$$

Consider now that the rectangular pulse $\langle a_p, T_p \rangle$ is strong enough to bring the block at the verge of overturning ($\theta(t = \text{large}) = \alpha$, $\dot{\theta}(t = \text{large}) = 0$). Given that the limit state at the verge of overturning happens after a very large time when compared with the duration of the pulse, T_p , the duration of the pulse can be assumed zero when compared with the time needed to reach the limit state. Accordingly, within the very large time scale of the limiting equilibrium, the angular velocity $\dot{\theta}(t = T_p)$ given by (40) can be assumed as $\dot{\theta}(t = 0)$. With this consideration, and after dropping the minus sign in front of the right-hand side of Eq. (40)—which is merely associated with the direction of shaking—the equation of the right-hand sides of Eqs. (40) and (39) gives:

$$\alpha = p \sin \alpha \left(\frac{a_p}{g \tan \alpha} - 1 \right) T_p \quad (41)$$

For slender blocks, $\alpha = \sin \alpha$ and Eq. (41) gives

$$\tan \alpha = \frac{a_p}{g} \frac{p T_p}{1 + p T_p} \quad (42)$$

Consequently, when a free-standing block with size R ($p = \sqrt{\frac{3g}{4R}}$) is subjected to a rectangular acceleration pulse with amplitude a_p and duration T_p , the condition for the block to remain stable is $\tan \alpha > \frac{a_p}{g} \frac{p T_p}{1 + p T_p}$.

Eq. (42) which was derived by using first principles of dynamics has the same form as Eq. (28) that was extracting by fitting the minimum overturning acceleration spectra computed numerically. The only difference is that the unity in the denominator of Eq. (42) that is derived for a rectangular acceleration pulse is replaced in Eq. (28) with $\gamma = \pi/3$ for a Type-A and a Type-C pulses or $\gamma = \pi/2$

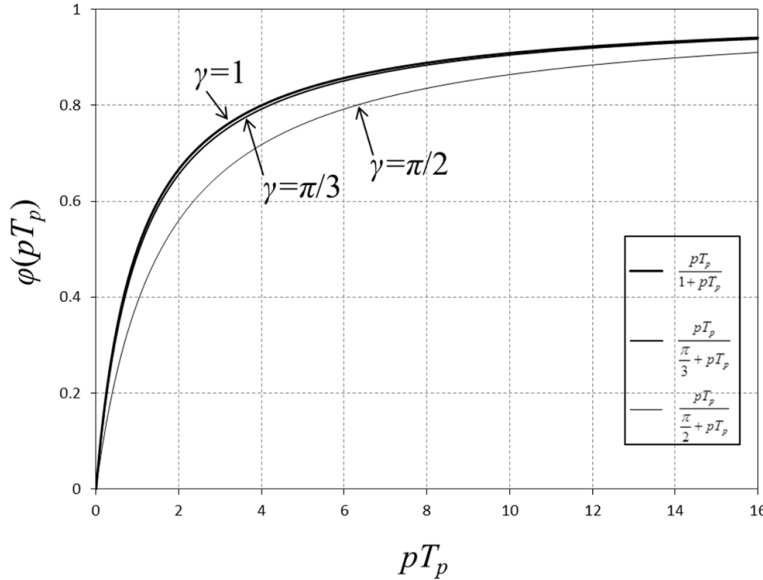


Fig. 8 Values of the function $\varphi(pT_p)$ that offer the minimum design slenderness (Eq. 37) as a function of the dimensionless product $\Pi_\omega = pT_p$

for a Type-B pulses. Fig. 8 plots the function $\varphi(pT_p) = \frac{pT_p}{\gamma + pT_p}$ for $\gamma=1$, $\pi/3$ and $\pi/2$. Given that the rectangular acceleration pulse has the strongest overturning potential among all other physically realizable pulses with equal duration the heavy dark line for $\gamma=1$ in Fig. 8 is above the minimum-slenderness lines as extracted from the corresponding overturning spectra. Accordingly, in the interest of safety the heavy dark line for $\gamma=1$ is recommended as a design curve to size the slenderness of free-standing object with a known height (given p).

9. The Dynamics of the Rocking Frame

While Fig. 7 illustrates the ample dynamic stability of a slender free-standing column as its size increases (large values of ω_p/p), the concept of rocking isolation becomes attractive and implementable once the dynamics of the rocking frame like the one shown in Fig. 1 (right) or Fig. 2 is delineated and explained to the extent that it can be easily used by the design engineers.

Results on the dynamic response of two free-standing columns capped with a freely supported beam have been presented by Allen et al. (1986), after adopting a Lagrangian formulation. In the Allen et al. (1986) paper it was assumed that the mass of each column, m_c , is much less than the mass of the freely supported beam, m_b , and therefore, the equation of motion derived was for $m_b/m_c \rightarrow \infty$. Furthermore, the results presented were obtained by solving the linearized equation of motion. It is worth noting that while the governing equation for the rocking frame appearing in the Allen et al. (1986) paper shows clearly that the response involves the slenderness, α , and size, R ,

of the columns of the rocking frame, the Allen et al. (1986) paper does not make any attempt to associate the dynamic response/stability of the rocking frame with that of the solitary rocking column.

In an effort to explain the seismic stability of ancient free-standing columns that support heavy epistles together with the even heavier frieze atop, Makris and Vassiliou (2013) studied the planar rocking response of an array of free-standing columns capped with a freely supported rigid beam as shown in Fig. 9.

The free-standing rocking frame shown in Fig. 9 is a single DOF structure with size $R = \sqrt{b^2 + h^2}$ and slenderness $\alpha = \tan(b/h)$. The only additional parameter that influences the dynamics of the rocking frame is the ratio of the mass of the cap beam, m_b , to the mass of all the N rocking columns, m_c , $\gamma = m_b/Nm_c$. For the Temple of Apollo in Corinth where the frieze is missing, γ is as low as 0.3, whereas in prefabricated bridges, $\gamma > 4$. As in the case of the single rocking column, the coefficient of friction is large enough so that sliding does not occur at the pivot point at the base and at the cap beam. Accordingly, the horizontal translation displacement $u(t)$ and the vertical lift $v(t)$ of the cap beam are functions of the single DOF $\theta(t)$. Following a variational formulation Makris and Vassiliou (2013) showed that the equation of motion of the rocking frame shown in Fig. 9 is

$$\ddot{\theta}(t) = -\frac{1+2\gamma}{1+3\gamma} p^2 \left(\sin[\alpha \operatorname{sgn}[\theta(t)] - \theta(t)] + \frac{\ddot{u}_g(t)}{g} \cos[\alpha \operatorname{sgn}[\theta(t)] - \theta(t)] \right) \quad (43)$$

Eq. (43), which describes the planar motion of the free-standing rocking frame, is precisely the same as Eq. (5), which describes the planar rocking motion of a single free-standing rigid column

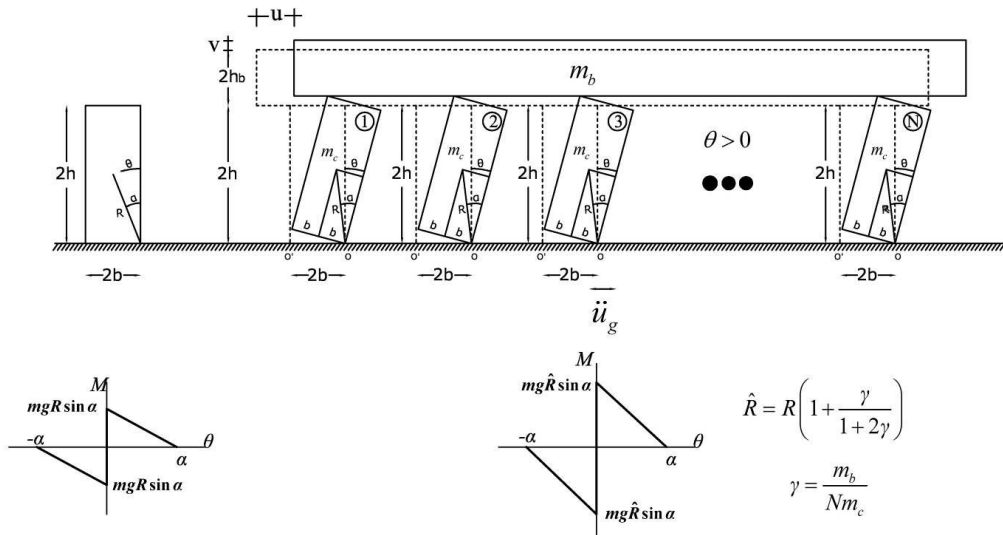


Fig. 9 The free-standing rocking frame with columns having size R and slenderness α is more stable than the solitary free-standing column shown on the left having the same size and slenderness

with the same slenderness α , except that in the rocking frame, the term p^2 is multiplied with the factor $(1 + 2\gamma)/(1 + 3\gamma)$. Accordingly, the frequency parameter of the rocking frame, \hat{p} , is

$$\hat{p} = \sqrt{\frac{1+2\gamma}{1+3\gamma}} p \quad (44)$$

where $p = \sqrt{3g/4R}$ is the frequency parameter of the solitary rocking column and $\gamma = m_b/Nm_c$ is the mass of the cap beam to the mass of all N columns.

For a light cap beam ($\gamma = m_b/Nm_c \rightarrow 0$), the multiplication factor $(1 + 2\gamma)/(1 + 3\gamma) \rightarrow 1$ and the array of free-standing columns coupled with a light epistyle exhibit precisely the dynamic rocking response of the solitary free-standing column. On the other hand, as the mass of the epistyle increases,

$$\lim_{\gamma \rightarrow \infty} \frac{1+2\gamma}{1+3\gamma} = \frac{2}{3} \quad (45)$$

According to Eq. (43), the rocking response and stability analysis of the free-standing rocking frame with columns having slenderness, α , and size, R , is described by all the past published work on the rocking response of the free-standing single block (Housner 1963, Yim et al. 1980, Aslam et al. 1980, Ishiyama 1982, Spanos and Koh 1984, Zhang and Makris 2001, Makris and Konstantinidis 2003, Vassiliou and Makris 2012, Dimitrakopoulos and DeJong 2012, among others), where the block has the same slenderness, α , and a larger size \hat{R} given by

$$\hat{R} = \frac{1+3\gamma}{1+2\gamma} R = \left(1 + \frac{\gamma}{1+2\gamma}\right) R \quad (46)$$

The remarkable result offered by Eq. (43) – that the heavier the cap beam is, the more stable is the free-standing rocking frame despite the rise of the center of gravity of the cap beam – has been also confirmed by the author after obtaining Eq. (43) for a pair of columns with the algebraically intense direct formulation after deriving the equations of motion of the two-column frame through dynamic equilibrium (Makris and Vassiliou 2014). Furthermore, numerical studies with the discrete element method by Papaloizou and Komodromos (2009) concluded to the same result – that the planar response of free-standing columns supporting epistyles is more stable than the response of the solitary, free-standing column. This finding has also been confirmed in the experimental studies of Mouzakis et al. (2002), Drosos et al. (2012) and Drosos and Anastasopoulos (2014a,b). Fig. 10 summarizes the increasing seismic stability as we go from the solitary free-standing column to the free-standing rocking frame.

During rocking motion of a free standing frame, the moment-rotation curve follows the curve shown in Fig. 9 (bottom) without enclosing any area. Energy is lost during impact when the angle of rotation reverses. At this instant it is assumed that the rotation continues smoothly and that the impact forces are concentrated at the new pivot points. Application of the angular momentum-impulsive theorem in association with the change of the linear momentum of the cap-beam (Makris and Vassiliou 2013) offers the ratio of the kinetic energy of the rocking frame after and before impact

$$r = \left(\frac{\dot{\theta}_2}{\dot{\theta}_1} \right)^2 = \left(\frac{1 - \frac{3}{2} \sin^2 \alpha + 3\gamma \cos 2\alpha}{1 + 3\gamma} \right)^2 \quad (47)$$

Eq. (47) indicates that the maximum coefficient of restitution, \sqrt{r} , of the rocking frame that is needed to engage into rocking motion is always smaller (therefore more energy is dissipated) than the maximum coefficient of restitution of the solitary column $= 1 - \frac{3}{2} \sin^2 \alpha$ (Housner 1963), which is recovered when $\gamma = m_b/2m_c = 0$.

The ample seismic stability of the free-standing rocking frame is shown by considering the two-column bent shown in Fig. 11 where its moment-rotation curve follows a negative slope as shown at the bottom of Fig. 10. Sliding at the pivot point during impact is prevented with a recess at the pile-cap and the cap-beam as shown in Fig. 11. In this numerical example, the cylindrical piers of the free-standing bridge bent are 9.6m tall with a diameter $d=2b=1.6m$. These are typical

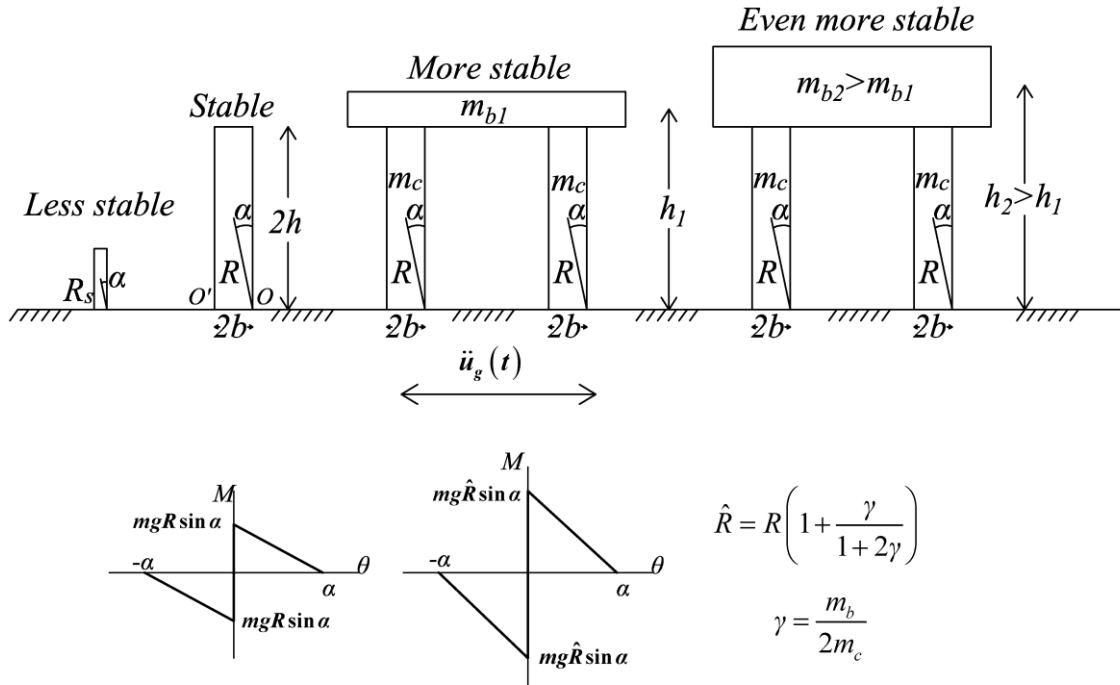


Fig. 10 The large free-standing column with size R and slenderness α is more stable than the geometrically similar smaller column shown at the far left of the figure. The free-standing rocking frame with columns having the same size R and same slenderness α is more stable than the solitary rocking column. A heavier freely supported cap-beam renders the rocking frame even more stable regardless of the rise of the center of gravity of the system

dimensions of bridge piers for highway overpasses and other bridges in the USA and Europe. Taller bridge piers with the same aspect ratio will result to even more stable configurations. With $2h=9.6m$ and $2b=1.6m$ the slenderness of the bridge pier is $\tan\alpha=b/h=1/6=0.167$ and its frequency parameter $p=\sqrt{\frac{3g}{4R}}=1.23$. Depending on the length of the adjacent spans and the per-length weight of the deck, the mass ratio $\gamma=\frac{m_b}{2m_c}$ assumes values from 4 and above ($\gamma \geq 4$). By adopting the low-end value of $\gamma=4$, the corresponding frequency parameters of the frame is $\hat{p}=\sqrt{\frac{1+2\gamma}{1+3\gamma}}p=0.832p \approx 1\text{ rad/s}$.

Consider now that the frame is subjected to a strong ground motion that contains a distinguishable pulse similar to those shown in Fig. 4 or Fig. 7. Let us assume that the period of the long duration pulse is $T_p=1\text{s}$, which is a rather long period (Bertero et al. 1978, Hall et al. 1995, Makris and Chang 2000, Baker 2007, Vassiliou and Makris 2011 among others). With $T_p=1\text{s}$ ($\omega_p=6.28\text{rad/s}$), the dimensionless product $\Pi_\omega=\frac{\omega_p}{p}=6.28$. According to the minimum overturning acceleration spectra shown in Fig. 7, which are for $\alpha=10^\circ$, for either a symmetric or antisymmetric Ricker pulse the dimensionless overturning acceleration Π_g/Π_α is larger than six ($\frac{\Pi_g}{\Pi_\alpha}=\frac{a_p}{g\tan\alpha}>6$);

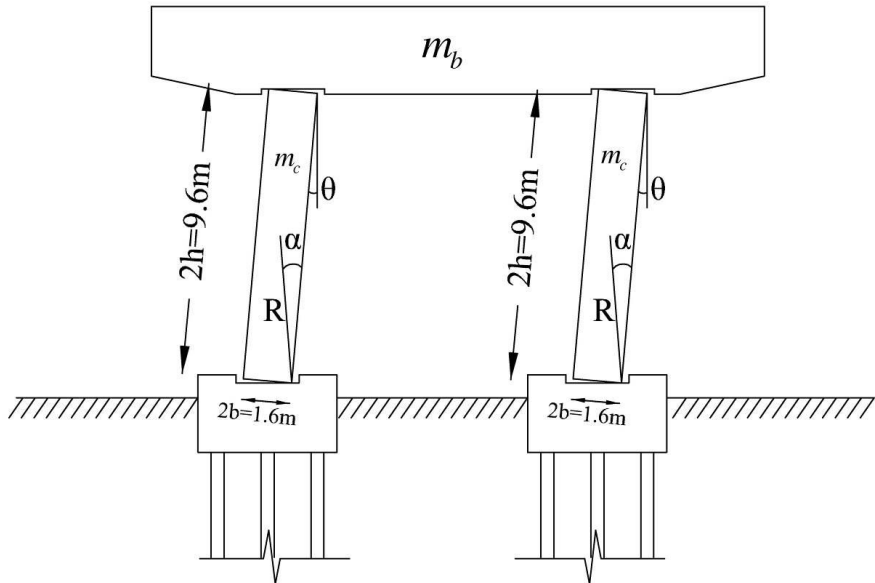


Fig. 11 Free-standing rocking bridge bent. Potential sliding during impact is prevented with the recess shown. No vertical post-tensioning, no continuation of the longitudinal reinforcement of the columns through the rocking interfaces at the pile-caps and the cap-beam. Its seismic resistance originates primarily from the mobilization of the rotational inertia of its piers

Consequently, when the rocking frame shown in Fig. 11 is excited by a Ricker pulse with $T_p=1.0\text{s}$, the minimum overturning acceleration amplitude of the pulse $a_p>6gtan\alpha$. For the rocking frame shown in Fig. 11, $\tan\alpha=1/6$; therefore $a_p>1\text{g}$ – which is a very high acceleration amplitude for a recorded pulse with duration $T_p=1\text{s}$. This illustrates the ample seismic stability of the free-standing rocking frame.

In the section above the seismic stability of the rocking frame (Fig. 11) has been shown by using as ground excitation strong pulses described either by symmetric or antisymmetric Ricker wavelets. The acceleration amplitude, a_p , and the duration, T_p , of any coherent acceleration pulse allow the use of dimensional analysis; and the derivation of the associated Π products presented in this work improves the understanding of the physics that govern the problem together with the organization and presentation of the response. Nevertheless, in an effort to further confirm the ample seismic stability of tall slender structures when subjected to strong recorded motions we report the results presented in Figs. 9-14 of Ishiyama's 1982 seminal paper. In this paper, Ishiyama (1982) shows that free-standing columns taller than 8m (800cm) and wider than 1m (100cm) survive the combine horizontal and vertical excitations of the May 15, 1940 El Centro Earthquake, the July 2, 1952 Taft Earthquake and the June 12, 1978 Miyagi-Oki Earthquake. Now the columns of the rocking frame shown in Fig. 11 are 9.6m (960cm) tall while they are 1.6m (160cm) wide; and according to Ishiyama's (1982) results they are most stable since the 160cm width of the column of the rocking frame is way beyond the scale of Ishiyama's graphs. The addition of the cap-beam on top of the columns renders the entire free-standing rocking frame even more stable.

Experimental studies on the dynamic response of the rocking frame (trilith) have been presented by Peña et al. 2008. In that study the slenderness of the columns is $\tan\alpha=2b/2h=0.22/0.8=0.275$ ($\alpha=15.38^\circ$), $R=\sqrt{(0.4\text{m})^2+(0.11\text{m})^2}=0.415\text{m}$, the frequency parameter of the columns, $p=4.21 \text{ rad/s}$ and $\gamma=\frac{265\text{kg}}{2\times 305\text{kg}}=0.434$. With these values the

frequency parameter of the rocking frame is $\hat{p}=\sqrt{\frac{1+2\gamma}{1+3\gamma}}p=0.9p=3.79\text{rad/s}$. Fig. 11 of Peña et al. 2008 paper plots response histories of the columns and cap-beam of the trilith when subjected to a constant sine excitation with amplitude $u_o=5\text{mm}=0.005\text{m}$ and frequency $f=3.3\text{Hz}$. With these values the amplitude of the base excitation is $\ddot{u}_{go}=u_o(2\pi f)^2=2.15\text{m/s}^2=0.219\text{g}$. Accordingly, the peak base excitation $\ddot{u}_{go}=0.219\text{g}$ is smaller than $g\tan\alpha=0.275\text{g}$ which is the minimum acceleration that is needed for uplifting of the rocking frame (see Eq. (43) or Makris and Vassiliou (2013) for a formal derivation with the principle of virtual work).

Given that $\ddot{u}_{go}=0.219\text{g}<g\tan\alpha=0.275\text{g}$, the trilith tested by Peña et al. 2008 apparently did not experience a pure rocking motion; but rather it experienced an inferior vibration mode due to possible minor anomalies of the contact surfaces. It is possible that these anomalies are responsible for the highly three dimensional behavior of the rocking frame that was recorded by Peña et al 2008. Given that such anomalies may be present to future implementations of the concept of the rocking frame, the potential sliding during impact can be prevented with the creation of a recess as shown in Fig. 11.

10. The Emerging Concept of Rocking Isolation for Bridges

The concept of allowing the piers of tall bridges to rock is not new. For instance, the beneficial effects that derive from uplifting and rocking have been implemented since the early 1970s in the South Rangitikei Bridge in New Zealand (Beck and Skinner 1971). Nevertheless, despite the successful design of the South Rangitikei bridge and the ample dynamic stability of the rocking frame as documented in Fig. 7 in association with Eq. (43) and further confirmed by numerical and experimental studies (Ishiyama 1982, Psycharis et al. 2003, Papaloizou and Komodromos 2009, Mouzakis et al. 2002, Drosos et al. 2012, Drosos and Anastopoulos 2014a,b) most modern tall bridges (with tall slender piers) are protected from seismic action via base (shear) isolation of the deck, rather than via (the most natural) rocking isolation. Part of the motivation of this work is to show in the simplest possible way that in the event that a rocking system is selected, the heavy deck atop the tall slender columns not only does not harm the stability of the columns but in contrast enhances the stability of the entire rocking system as shown by Eq. (43).

This work comes to support the emerging design concept (mainly advanced by the prefabricated bridge technology) of concentrating the inelastic deformations of bridge frame at the locations where the bridge-piers meet the foundation and the deck (Mander and Cheng 1997, Sakai and Mahin 2004, Wacker et al. 2005, Mahin et al. 2006, Cheng 2008, Cohagen et al. 2008, Yamashita and Sanders 2009, Barthès et al. 2010, among others). It shall however be stressed that in the prefabricated bridge technology, the bridge piers and the deck are not free standing, therefore, the structural system is essentially a hybrid system in-between the rocking frame examined in this work and a traditional ductile moment-resisting frame.

In this hybrid system the bridge-piers are connected to their foundation and the deck with a post-tensioned tendon that passes through the center-axis of the piers, together with longitudinal mild-steel reinforcement which runs near their outer surface. With this design, in most times the initial negative stiffness (see Fig. 3 bottom) of the rocking frame is eliminated and altered to a positive quantity; therefore, the behavior of prefabricated bridge frames has very little in common with the behavior of truly rocking frames and they merely behave as traditional inelastic structures where forces and deformations are estimated with the equivalent static lateral force procedure. Accordingly, in the hybrid system, most of the appreciable seismic stability that is associated with rocking (see Fig. 7) is eradicated. Furthermore, during seismic shaking the post-tensioned, prefabricated bridge frame may be subject to resonance due to its overall positive stiffness; while, the longitudinal mild-steel reinforcement that extends through the seismic connection is subject to buckling and fracture.

At present, the equivalent static lateral force procedure is deeply rooted in the design philosophy of the structural engineering community which is primarily preoccupied on how to improve the ductility and performance of the seismic connections; while the ample dynamic rocking stability that derives from the beneficial coexistence of large rotational inertia, negative stiffness and gravity as described by Eq. (43) and documented in Fig. 7 is ignored. At the same time, it shall be recognized that during the last decade there have been several publications which have voiced the need to go beyond the elastic response spectrum and the associated equivalent static lateral force procedure (Makris and Konstantinidis 2003, Lagomarsino et al. 2004, Apostolou et al. 2007, Resemini et al. 2008, Anastopoulos et al. 2010, Dimitrakopoulos and DeJong 2012, among others). In addition to these studies, Acikgoz and DeJong (2012) and Vassiliou et al. (2013) have examined in depth the rocking response of flexible, slender structures

and the main conclusion is that the flexure of a tall rocking structure further increases its seismic stability. To this end, it is worth mentioning the recent theoretical work on the three-dimensional rocking response of free-standing columns (Konstantinidis and Makris 2007, Zulli et al. 2012, Chatzis and Smyth 2012a,b) which confirms the seismic stability of free-standing columns in three dimensions. The time is therefore ripe for the development of new, physically motivated response/design curves which are relevant (in a technically sound way) with the response/design of large, slender structures. Part of the motivation for this paper is to bring forward the ample seismic stability associated with the free rocking of large, slender structures and the corresponding rocking frame. The implementation of the proposed approach needs a systematic investigation of several pertinent practical issues such as the potential crushing of the pivoting points of the columns (Roh and Reinhorn 2010a,b) and the accommodation of the deck uplift at the end-abutments.

11. Conclusions

Half a century ago George Housner's 1963 seminal paper marked the beginning of a series of systematic studies on the dynamic response and stability of rocking structures which gradually led to the development of rocking isolation—an attractive practical and economical alternative for the seismic protection of tall, slender structures which originates from the mobilization of their large rotational inertia. Partly motivated from this 50-year anniversary, this paper builds upon selected past contributions in an effort to bring forward the major advances together with the unique advantages of rocking isolation.

After revisiting Housner's size-frequency scale effect for the solitary column which merely explains that when a free-standing column is sufficiently large it can survive any strong shaking, the paper builds upon a recent remarkable result—that the dynamic rocking response of an array of free-standing columns capped with a rigid beam is identical to the rocking response of a solitary column with the same slenderness; yet, with larger size, which is a more stable configuration (Eq. 46). Most importantly, the dynamics of the rocking frame reveals that the heavier the freely supported beam is, the more stable is the rocking frame regardless of the rise of the center of gravity of the cap beam, concluding that top-heavy rocking frames are more stable than when they are top-light.

This "counterintuitive" behavior renders rocking isolation a most attractive alternative for the seismic protection of bridges given that the heavier is the deck, the more stable is the rocking bridge. The realization of a truly rocking frame which can fully mobilize its rotational inertia with neither post-tensioning nor continuation of the longitudinal reinforcement through the rocking interfaces shall remove several of the concepts associated with the seismic connections of prefabricated bridges such as buckling and fracture of the longitudinal reinforcing bars or spallings of the concrete corners.

The ultimate aim of this paper is to bring forward the ample seismic stability that originates from the mobilization of the rotational inertia of free-standing structures and to offer the theoretical background in an effort to accept and establish rocking isolation and its associated hinging mechanism not only as a limit-state mechanism, but also as an operational state (seismic protection) mechanism for large, slender structures as was accepted more than 2.5 millennia ago by the builders of ancient temples as shown in Fig. 2.

Acknowledgments

Financial support for this study has been provided by the research project "SeismoRockBridge" which is implemented under the "ARISTEIA" Action of the "OPERATIONAL PROGRAMME EDUCATION AND LIFELONG LEARNING" and is co-funded by the European Social Fund (ESF) and Greek National Resources.

The assistance of Dr. H. Alexakis regarding the management of the electronic document is appreciated.

Data and Resources

The accelerograph data used in this study were collected from the website of PEER strong ground motion database at <http://peer.berkeley.edu> (last accessed September 2011).

References

- Acikgoz, S., and DeJong, M.J. (2012), "The interaction of elasticity and rocking in flexible structures allowed to uplift", *Earthq. Eng. Struct. Dynam.*, **41**, 2177-2194.
- Addison, P.S. (2002), *The Illustrated Wavelet Transform Handbook: Introductory Theory and Applications in Science, Engineering, Medicine and Finance*, Institute of Physics Handbook, London.
- Ajrab, J., Pekcan, G. and Mander, J. (2004), "Rocking wall-frame structures with supplemental tendon systems", *J. Struct. Eng.*, **130**, 895-903.
- Alavi, B. and Krawinkler, H. (2001), *Effects of Near-Source Ground Motions on Frame-Structures*, John A. Blume Earthquake Engineering Center Rept. No. 138, Stanford University
- Allen, R.H., Oppenheim, I.J., Parker, A.R. and Bielak, J. (1986), "On the dynamic response of rigid body assemblies", *Earthq. Eng. Struct. Dyn.*, **14**, 861-876.
- Anastasopoulos, I., Gazetas, G., Loli, M., Apostolou, M. and Gerolymos, N. (2010), "Soil failure can be used for seismic protection of structures", *Bull. Earthq. Eng.*, **8**, 309-326.
- Anooshehpoor, A., Heaton, T.H., Shi, B. and Brune, J.N. (1999), "Estimates of the ground acceleration at Point Reyes station during the 1906 San Francisco earthquake", *Bull. Seismol. Soc. Am.*, **89**, 843-853.
- Apostolou, M., Gazetas, G. and Garini, E. (2007), Seismic response of slender rigid structures with foundation uplift, *Soil Dyn. Earthq. Eng.*, **27**, 642-654.
- Aslam, M., Scalise, D.T. and Godden, W.G. (1980), Earthquake rocking response of rigid blocks, *J. Struct. Eng. Div. (ASCE)*, **106**, 377-392.
- Baker, W.J. (2007), "Quantitative classification of near fault ground motions using wavelet analysis", *Bull. Seism. Soc. Am.*, **97**, 1486-1501.
- Barenblatt, G.I. (1996), *Scaling, self-similarity, and intermediate asymptotics*, Cambridge University Press, Cambridge, U.K.
- Barthès, C., Hube, M. and Stojadinović, B. (2010), "Dynamics of post-tensioned rigid blocks", in *9th US & 10th Canadian Conference on Earthquake Engineering*, July 25-29, Toronto, Canada.
- Beck, J.L. and Skinner, R.I. (1974), The seismic response of a reinforced concrete bridge pier designed to step, *Earthq. Eng. Struct. Dyn.*, **2**, 343-358.
- Bertero, V.V., Mahin, S.A. and Herrera, R.A. (1978), "A seismic design implications of near-fault San Fernando earthquake records", *Earthq. Eng. Struct. Dyn.*, **6**, 31-42.
- Bertero, V.V., Anderson, J.C., Krawinkler, H. and Miranda, E. (1991), *Design guidelines for ductility and drift limits*, Rept. No. EERC/UCB-91/15, Earthquake Engineering Research Center, University of

- California, Berkeley, California.
- Chatzis, M.N. and Smyth, A.W. (2012a), "Modeling of the 3D rocking problem", *Int. J. Non-Linear Mech.*, **47**, 85-98.
- Chatzis, M.N. and Smyth, A.W. (2012b), "Robust modeling of the rocking problem", *J. Eng. Mech.*, **138**, 247-262.
- Cheng, C.T. (2008), "Shaking table tests a self-centering designed bridge substructure", *Eng Struct.*, **30**, 3426-3433.
- Cohagen, L., Pang, J.B.K., Stanton, J.F. and Eberhard, M.O. (2008), *A precast Concrete Bridge Bent Designed to Recenter after an Earthquake, Research Report*, Federal Highway Administration.
- Deng, L., Kutter, B. and Kunnath, S. (2012), "Centrifuge modeling of bridge systems designed for rocking foundations", *J. Geotech. Geoenviron. Eng.*, **138**, 335-344.
- Dimitrakopoulos, E.G. and DeJong, M.J. (2012), "Revisiting the rocking block: closed-form solutions and similarity laws", *Proceedings of the Royal Society A*, **468**, 2294-2318.
- Drosos, V., Anastasopoulos, I. and Gazetas, G. (2012), *Seismic Behavior of Classical Columns: An Experimental Study*, Laboratory of Soil Mechanics Research Report: LSM NTUA-12-01.
- Drosos, V. and Anastasopoulos, I. (2014a), "Shaking table testing of multidrum columns and portals", *Earthq. Eng. Struct. Dynam.* (published on line), Doi: 10.1002/eqe.2418
- Drosos, V. and Anastasopoulos, I. (2014b), "Experimental investigation of the seismic response of classical temple columns", *Bull. Earthquake Eng.* (published on line), Doi: 10.1007/s10518-014-9608-y
- Gajan, S., Hutchinson, T.C., Kutter, B.L., Raychowdhury, P., Ugalde, J.A. and Stewart, J.P. (2008), *Numerical Models for Analysis and Performance-Based Design of Shallow Foundations Subject to Seismic Loading*, Report No. PEER-2007/04, Pacific Earthquake Engineering Research Center, University of California, Berkeley.
- Gajan, S. and B. Kutter (2008), "Capacity, settlement, and energy dissipation of shallow footings subjected to rocking", *J. Geotech. Geoenviron. Eng.*, **134**, 1129-1141.
- Gelagoti, F., Kourkoulis, R., Anastasopoulos, I. and Gazetas, G. 2012), "Rocking isolation of low-rise frame structures founded on isolated footings", *Earthq. Eng. Struct. Dyn.*, **41**, 1177-1197.
- Hall, J.F., Heaton, T.H., Halling, M.W. and Wald, D.J. (1995), "Near-source ground motion and its effects on flexible buildings", *Earthq. Spectr.*, **11**, 569-605.
- Harden, C., Hutchinson, T. and Moore, M. (2006), Investigation into the Effects of Foundation Uplift on Simplified Seismic Design Procedures, *Earthq. Spectr.*, **22**, 663-692.
- Hogan, S.J. (1989), "On the dynamics of rigid-block motion under harmonic forcing", *Proceedings of the Royal Society A*, **425**, 441-476.
- Hogan, S.J. (1990), "The many steady state responses of a rigid block under harmonic forcing", *Earthq. Eng. Struct. Dyn.*, **19**, 1057-1071.
- Housner, G.W. (1963), The behaviour of inverted pendulum structures during earthquakes, *Bull. Seismol. Soc. Am.* **53**, 404-417.
- Hung, H.H., Liu, K.Y., Ho, T.H. and Chang, K.C. (2011), "An experimental study on the rocking response of bridge piers with spread footing foundations", *Earthq. Eng. Struct. Dynam.*, **40**, 749-769.
- Ikegami, R., and Kishinouye, F. (1947), "A study on the overturning of rectangular columns in the case of the Nankai earthquake on December 21, 1946", *Bull. Earthq. Res. Inst. Tokyo Univ.*, **25**, 49-55.
- Ikegami, R., and Kishinouye, F. (1950), "The acceleration of earthquake motion deduced from overturning of the gravestones in case of the Imaichi Earthquake on Dec. 26, 1949", *Bull. Earthq. Res. Inst. Tokyo Univ.*, **28**, 121-128.
- Ishiyama, Y. (1982), "Motions of rigid bodies and criteria for overturning by earthquake excitations", *Earthq. Eng. Struct. Dyn.*, **10**, 635-650.
- Karavasilis, T.L., Makris, N., Bazeos, N. and Beskos, D.E. (2010), "Dimensional response analysis of multistory regular steel MRF subjected to pulselike earthquake ground motions", *J. Struct. Eng.*, **136**, 921-932.
- Kawashima, K., Nagai, T. and Sakellaraki, D. (2007), "Rocking Seismic Isolation of Bridges Supported by

- Spread Foundations”, in *Proceedings of the 2nd Japan-Greece Workshop on Seismic Design, Observation and Retrofit of Foundations*, Japan Society of Civil Engineers, Tokyo, Japan, vol. 2, 254-265.
- Kirkpatrick, P. (1927), Seismic measurements by the overthrow of columns, *Bull. Seismol. Soc. Am.*, **17**, 95-109.
- Konstantinidis, D. and Makris, N. (2005), “Seismic response analysis of multidrum classical columns”, *Earthq. Eng. Struct. Dynam.*, **34** 1243-1270.
- Konstantinidis, D. and N. Makris (2007), The Dynamics of a Rocking Block in Three Dimensions, in *Proceedings of the 8th HSTAM International Congress on Mechanics*, July 12-14, Patras, Greece.
- Konstantinidis, D. and N. Makris (2010), Experimental and analytical studies on the response of 1/4-scale models of freestanding laboratory equipment subjected to strong earthquake shaking, *Bull. Earthquake Eng.*, **8** 1457-1477.
- Kounadis, A.N., Papadopoulos, G.J. and Cotovos, D.M. (2012), “Overturning instability of a two-rigid block system under ground excitation”, *J. Appl. Math. Mech.*, **92**, 536-557.
- Lagomarsino, S., S. Podestà, S. Resemini, E. Curti, and S. Parodi (2004), Mechanical models for the seismic vulnerability assessment of churches, in *Proceedings of IV SAHC*, Padova, Italy, A.A. Balkema, London (UK), vol. 2, 1091-1101.
- Mahin, S., J. Sakai, and H. Jeong (2006), “Use of partially prestressed reinforced concrete columns to reduce post-earthquake residual displacements of bridges”, in *Proceedings of the 5th National Seismic Conf. on Bridges & Highways*, San Francisco.
- Makris, N. (1997), “Rigidity–plasticity–viscosity: can electrorheological dampers protect base-isolated structures from near-source ground motions?”, *Earthq. Eng. Struct. Dyn.*, **26**, 571-591.
- Makris, N., and Y. Roussos (1998), *Rocking response and overturning of equipment under horizontal pulse-type motions*. Rep. No. PEER-98/05, Pacific Earthquake Engrg. Res. Ctr., University of California, Berkeley, California
- Makris, N., and Y. Roussos (2000), “Rocking response of rigid blocks under near-source ground motions”, *Geotech. Lond.*, **50**, 243-262.
- Makris, N. and Chang, S.P. (2000), “Effect of viscous, viscoplastic and friction damping on the response of seismic isolated structures”, *Earthq. Eng. Struct. Dyn.*, **29**, 85-107.
- Makris, N. and Konstantinidis, D. (2003), The rocking spectrum and the limitations of practical design methodologies, *Earthq. Eng. Struct. Dyn.*, **32**, 265-289.
- Makris, N. and Black, C.J. (2004a), Dimensional analysis of rigid-plastic and elastoplastic structures under pulse-type excitations, *J. Eng. Mech. (ASCE)*, **130**, 1006-1018.
- Makris, N. and Black, C.J. (2004b), “Dimensional analysis of bilinear oscillators under pulse-type excitations”, *J. Eng. Mech. (ASCE)*, **130**, 1019-1031.
- Makris, N. and Vassiliou, M.F. (2012), “Sizing the slenderness of free-standing rocking columns to withstand earthquake shaking”, *Arch. Appl. Mech.*, **82**, 1497-1511.
- Makris, N. and Vassiliou, M.F (2013), “Planar rocking response and stability analysis of an array of free-standing columns capped with a freely supported rigid beam”, *Earthq. Eng. Struct. Dynam.*, **42**, 431-449.
- Makris, N. and Vassiliou, M.F (2014), “Are Some Top-Heavy Structures More Stable?”, *J. Struct. Eng.*, **140**, Doi: 10.1061/(ASCE)ST.1943-541X.0000933
- Mander, J.B. and Cheng, C-T.(1997), *Seismic Resistance of Bridge Piers Based on Famage Avoidance Design*, Tech. Rep. No. NCEER- 97-0014, National Center for Earthquake Engineering Research, Dept. of Civil and Environmental Engineering, State Univ. of New York, Buffalo, N.Y.
- MATLAB (2002), High-performance Language of Technical Computing. The Mathworks, Inc., Natick, MA
- Mavroelidis, G.P., and Papageorgiou, A.S. (2003), “A mathematical representation of near-fault ground motions”, *Bull. Seismol. Soc. Am.*, **93**, 1099-1131.
- Milne, J. (1885), Seismic experiments. *Trans. Seismol. Soc. Jpn.*, **8**, 1-82.
- Mouzakis, H.P., Pscharis, I.N., Papastamatiou, D.Y., Carydis, P.G., Papantonopoulos, A.C. and Zambas, C. (2002), “Experimental investigation of the earthquake response of a model of a marble classical column”, *Earthq. Eng. Struct. Dyn.*, **31**, 1681-1698.

- Muto, K., Umemure, H. and Sonobe, Y. (1960), "Study of the overturning vibration of slender structures", in *Proceedings of the second world conference on Earthquake Engineering*, Japan 1960, 1239-1261.
- Palmeri, A. and Makris, N. (2008), "Linearization and first-order expansion of the rocking motion of rigid blocks stepping on viscoelastic foundation", *Earthq. Eng. Struct. Dyn.*, **37**, 1065-1080.
- Papaloizou, L. and Komodromos, K. (2009), "Planar investigation of the seismic response of ancient columns and colonnades with epistyles using a custom-made software", *Soil Dyn. Earthq. Eng.*, **29**, 1437-1454.
- Peña, F., Lourenço, P.B. and Campos-Costa, A. (2008), "Experimental dynamic behavior of free-standing multi-block structures under seismic loadings", *J. Earthq. Eng.*, **12**, 953-979.
- Pompei, A., Scalia, A. and Sumbatyan, M.A. (1998), "Dynamics of rigid block due to horizontal ground motion", *J. Engrg. Mech. (ASCE)*, **124**, 713-717.
- Pscharis, I.N. and Jennings, P.C. (1983), "Rocking of slender rigid bodies allowed to uplift", *Earthq. Eng. Struct. Dynam.*, **11**, 57-76.
- Pscharis, I.N. (1990), "Dynamic behaviour of rocking two-block assemblies", *Earthq. Eng. Struct. Dynam.*, **19**, 555-575.
- Pscharis, I.N., J.V. Lemos, Papastamatiou, D.Y. and Zambas, C. (2003), "Numerical study of the seismic behaviour of a part of the Parthenon Pronaos", *Earthq. Eng. Struct. Dynam.*, **32**, 2063-2084.
- Resemini S., Lagomarsino, S. and Cauzzi, C. (2008), "Dynamic response of rocking masonry elements to long period strong ground motion", in *Proceedings of the 14th World Conference on Earthquake Engineering*, October 12-17, Beijing, China.
- Ricker, N. (1943), "Further developments in the wavelet theory of seismogram structure", *Bull. Seismol. Soc. Am.*, **33**, 197-228.
- Ricker, N. (1944), "Wavelet functions and their polynomials", *Geophysics*, **9**, 314-323.
- Roh, H. and Reinhorn, A. (2010a), "Modeling and seismic response of structures with concrete rocking columns and viscous dampers", *Eng. Struct.*, **32**, 2096-2107.
- Roh, H. and Reinhorn, A. (2010b), "Nonlinear static analysis of structures with rocking columns", *J. Struct. Eng.*, **136**, 532-542.
- Sakai, J. and Mahin, S. (2004), *Analytical Investigations of New Methods for Reducing Residual Displacements of Reinforced Concrete Bridge Columns*, PEER Report 2004/02, Pacific Earthquake Engineering Research Center, University of California, Berkeley, California.
- Scalia, A. and Sumbatyan, M.A. (1996), "Slide rotation of rigid bodies subjected to a horizontal ground motion", *Earthq. Eng. Struct. Dynam.*, **25**, 1139-1149.
- Shenton, H.W (1996), "Criteria for initiation of slide, rock, and slide-rock rigid-body modes", *J. Engrg. Mech. (ASCE)*, **122**, 690-693.
- Shi, B., Anooshehpoor, A., Zeng, Y. and Brune, J.N. (1996), "Rocking and overturning of precariously balanced rocks by earthquake", *Bull. Seismol. Soc. Am.*, **86**, 1364-1371.
- Sinopoli, A. (1989), Kinematic approach in the impact problem of rigid bodies, *Applied Mechanics Reviews (ASME)*, **42**, S233-S244
- Somerville, P. and Graves, R. (1993), "Conditions that give rise to unusually large long period ground motions," *Struct. Design Tall Buildings*, **2**, 211-232.
- Spanos, P.D. and Koh, A.S. (1984), Rocking of rigid blocks due to harmonic shaking, *J. Engrg. Mech. (ASCE)*, **110**, 1627-1642.
- Spanos, P.D., Roussis, P.C. and Politis, N.P.A. (2001), "Dynamic analysis of stacked rigid blocks", *Soil Dyn. Earthq. Eng.*, **21**, 559-578.
- Taniguchi, T. (2002), "Non-linear response analyses of rectangular rigid bodies subjected to horizontal and vertical ground motion", *Earthq. Eng. Struct. Dyn.*, **31**, 1481-1500.
- Tso, W.K. and Wong, C.M. (1989a), "Steady state rocking response of rigid blocks Part 1: Analysis", *Earthq. Eng. Struct. Dynam.*, **18**, 89-106.
- Tso, W.K. and Wong C.M. (1989b), "Steady state rocking response of rigid blocks Part 2: Experiment", *Earthq. Eng. Struct. Dynam.*, **18**, 107-120.

- Vassiliou, M.F. and Makris, N. (2011), "Estimating time scales and length scales in pulselike earthquake acceleration records with wavelet analysis", *Bull. Seismol. Soc. Am.*, **101**, 596-618.
- Vassiliou, M.F. and Makris, N. (2012), "Analysis of the rocking response of rigid blocks standing free on a seismically isolated base", *Earthq. Eng. Struct. Dynam.*, **41**, 177-196.
- Vassiliou, M.F., Mackie, K.R. and Stojadinović, B. (2013), "Rocking response of slender, flexible columns under pulse excitation", in *Proceedings of the 4th ECCOMAS Thematic Conference on Computational Methods in Structural Dynamics and Earthquake Engineering*, 12-14 June, Kos Island, Greece, Paper No. C 1084.
- Veletsos, A.S., Newmark, N.M. and Chelepati, C.V. (1965), "Deformation spectra for elastic and elastoplastic systems subjected to ground shock and earthquake motions", in *Proceedings of the 3rd World Conference on Earthquake Engineering*, vol. II, 663-682, Wellington, New Zealand.
- Wacker, J.M., Hieber, D.G., Stanton, J.F. and Eberhard, M.O. (2005), *Design of Precast Concrete piers for Rapid Bridge Construction in Seismic Regions*, Research Report, Federal Highway Administration
- Yamashita, R., and Sanders, D. (2009), "Seismic performance of precast unbonded prestressed concrete columns", *ACI Struct. J.*, **106**, 821-830.
- Yim, C.S., Chopra, A.K. and Penzien, J. (1980), "Rocking response of rigid blocks to earthquakes", *Earthq. Eng. Struct. Dynam.*, **8**, 565-587.
- Zhang, J., and Makris, N. (2001), "Rocking response of free-standing blocks under cycloidal pulses", *J. Engrg. Mech. (ASCE)*, **127**, 473-483.
- Zulli, D., Contento, A. and Di Egidio, A. (2012), "3D model of rigid block with a rectangular base subject to pulse-type excitation", *Int. J. Non-Linear Mech.*, **47**, 679-687.